Intracellular *Salmonella* Paratyphi A is motile and differs in the expression of flagella-chemotaxis, SPI-1 and carbon utilization pathways in comparison to Intracellular *S*. Typhimurium

Helit Cohen[1,†], Claire Hoede[2,†], Felix Scharte[3,†], Charles Coluzzi[4], Emiliano Cohen[1], Inna Shomer[1], Ludovic Mallet[2], Remy Felix Serre[5], Thomas Schiex[6], Isabelle Virlogeux-Payant[7], Guntram Grassl[8], Michael Hensel[3,9§], Hélène Chiapello[2,4,§], Ohad Gal-Mor[1,10,§]

[1] The Infectious Diseases Research Laboratory, Sheba Medical Center, Tel-Hashomer, Israel

[2] INRAE, UR875 Applied Mathematics and Computer Science Toulouse (MIAT), Platform GenoToul Bioinfo, F-31326 Castanet-Tolosan, France

[3] Abt. Mikrobiologie, Universität Osnabrück, Osnabrück, Germany

[4] Université Paris-Saclay, INRAE, MaIAGE, 78350 Jouy-en-Josas, France

[5] INRAE, GeT-PlaGe, Genotoul, 31326 Castanet-Tolosan, France

[6] Université Fédérale de Toulouse, ANITI, INRAE, UR 875, Toulouse, France

[7] INRAE, Université de Tours, UMR ISP, F-37380, Nouzilly, France

[8] Institute of Medical Microbiology and Hospital Epidemiology, Hannover Medical School and German Center for Infection Research (DZIF), Hanover, Germany

[9] CellNanOs – Center of Cellular Nanoanalytics Osnabrück, Universität Osnabrück, Osnabrück, Germany

[10] Department of Clinical Microbiology and Immunology, Faculty of Medicine, Tel-Aviv University, Tel-Aviv, Israel

† Equal contribution

§ Corresponding authors

ABSTRACT

Although *Salmonella* Typhimurium (STM) and *Salmonella* Paratyphi A (SPA) belong to the same phylogenetic species, share large portion of their genome and express many common virulence factors, they differ vastly in their host specificity, the immune response they elicit, and the clinical manifestations they cause. In this work, we compared for the first time their intracellular trascriptomic architecture and cellular phenotypes during epithelial cell infection. While transcription induction of many metal transport systems, purines, biotin, PhoPQ and SPI-2 regulons was common in both intracellular SPA and STM, we identified 234 differentially expressed genes that showed distinct expression patterns in intracellular SPA vs. STM. Surprisingly, clear expression differences were found in SPI-1, motility and chemotaxis, and carbon (mainly citrate, galactonate and ethanolamine) utilization pathways, indicating that these pathways are regulated and possibly function differently, during their intracellular phase. Moreover, we show that the induction of flagella genes by intracellular SPA leads to cytosolic motility, a conserved trait specific to SPA. To the best of our knowledge, this is the first report of a flagellum-dependent intracellular motility of any *Salmonella* serovar in living host cells. Importantly, we demonstrate that the elevated expression of SPI-1 and motility genes by intracellular SPA results in increased invasiveness of SPA, following exit from host cells. We propose that such changes prime SPA towards new cycles of host cell infection and contribute to the ability of SPA to disseminate beyond the intestinal lamina propria of the human host, during enteric fever.

IMPORTANCE

Salmonella enterica is a ubiquitous, facultative intracellular animal and human pathogen. Although non-typhoidal *Salmonella* (NTS) and typhoidal *Salmonella* serovars belong to the same phylogenetic species and share many virulence factors, the disease they cause in humans is very different. While the underlying mechanisms for these differences are not fully understood, one possible reason expected to contribute to their different pathogenicity is a distinct expression pattern of genes involved in host-pathogen interactions. Here, we compared the global gene expression and the intracellular behavior, during epithelial cell infection of *S*. Paratyphi A (SPA) and *S*. Typhimurium (STM), as prototypical serovars of typhoidal and NTS, respectively. Interestingly, we identified different expression patterns in key virulence and metabolic pathways, together with intracellular motility and increased invasiveness of SPA, following exit from infected cells. We hypothesize that these differences are pivotal to the invasive and systemic disease developed following SPA infection in humans.

INTRODUCTION

Salmonella enterica (*S. enterica*) is an abundant Gram-negative, facultative intracellular animal and human pathogen. This highly diverse bacterial species contains more than 2600 antigenically distinct serovars (biotypes) that are different in their host specificity and the disease they cause. The developed clinical manifestation is the result of multiple factors, but largely depends on the characteristics of the infecting serovar and the immunological status of the host (1). Many of the *S. enterica* serovars, including the ubiquitous *S. enterica* serovar Typhimurium (*S.* Typhimurium) are generalist pathogens and are capable of infecting a broad range of host species. Infection of immunocompetent humans by non-typhoidal *Salmonellae* (NTS) typically leads to a self-limiting, acute inflammatory gastroenteritis, confined to the terminal ileum and colon. In contrast, a few serovars including Typhi, Paratyphi A and Sendai, collectively referred to as 'typhoidal salmonellae' are restricted to the human host and known as the causative agents of enteric (typhoid) fever. In most cases, enteric fever is a non-inflammatory, systemic life-threatening disease, presented as bacteremia and dissemination of the pathogen to systemic sites such as the spleen, liver and lymph nodes (2-4).

S. enterica infections are still considered a significant cause of mortality and morbidity with an annual incidence of over 27 million cases of enteric fever (5), and 78.7 million cases of gastroenteritis (6) worldwide. In recent years, the global prevalence of *S.* Paratyphi A (SPA) is increasing and in some countries (especially in eastern and southern Asia), SPA infections are accountable for up to 50% of all enteric fever cases (7, 8). The lack of a commercial SPA vaccine and the increased occurrence of antibiotic resistant strains illuminate SPA as a significant public health concern that is still an understudied pathogen (9).

Active invasion into eukaryotic non-phagocytic cells is one of the key virulence-associated phenotypes of all *S. enterica* serovars. This unique capability facilitates *Salmonella* intestinal epithelium

crossing of the small intestine (10) and is mediated by a designated type three secretion system (T3SS) encoded in the *Salmonella* Pathogenicity Island (SPI)-1. This sophisticated syringe-like nanosystem is evolutionary related to the flagellar apparatus (11) and used to translocate an array of effector proteins directly into the host cell cytoplasm. Translocated effectors by T3SS-1 trigger cytoskeletal rearrangements and *Salmonella* penetration of intestinal barriers (12). In addition, T3SS-1 and its associated effectors significantly contribute to intestinal inflammation (13) that helps *Salmonella* to compete with the gut microbiota (14).

After penetrating the lamina propria into the submucosa and mesenteric lymph nodes, *Salmonella* are taken up by phagocytic cells such as macrophages and dendritic cells. Within host cells, *Salmonella* are compartmentalized into a modified intracellular phagosome, known as the *Salmonella* containing vacuole (SCV). Inside the SCV *Salmonella* manipulates the phagosome-lysosome membrane fusion and other cellular pathways, and starts to replicate intracellularly (13). These activities require a second T3SS encoded by genes on SPI-2 and the translocation of a distinct set of effectors proteins (15).

Typhoid fever disease and host-response to *S*. Typhi infection is largely attributed to the function of the Vi polysaccharide capsule and its associated regulator, TviA encoded on SPI-7 (16-19). Nonetheless, since SPA does not harbor the SPI-7, nor expresses the Vi capsule, different mechanisms are expected to contribute to the clinically indistinguishable enteric fever disease caused by SPA and *S*. Typhi. Previously, we showed that in *Salmonella* culture grown in LB to the late logarithmic phase, SPI-1 genes and T3SS-1 effectors are expressed and secreted at significantly lower levels by SPA compared to *S*. Typhimurium (STM) (20), and demonstrated differences in the regulatory setup of the flagella-chemotaxis pathway between these serovars (21, 22).

Here, to further understand the different pathogenicity of SPA vs. STM as prototypic NTS, we set out to compare their transcriptional architecture, during non-phagocytic host cell infection. Surprisingly,

in sharp contrast to the expression pattern in LB grown culture, we show that intracellular SPA is motile and induces the expression of SPI-1 and flagellar genes, compared to intracellular STM. In addition, we demonstrate that SPA and STM diverge in the intracellular expression of genes for citrate and ethanolamine metabolism and in their ability to utilize these carbon sources in vitro. We hypothesize that these differences are pivotal for the distinct diseases resulting from SPA vs. STM infection, and their different interactions with the human host.

RESULTS

The intracellular transcriptomic landscape of *S*. Typhimurium

Although STM and SPA belong to the same species, share about 89 % of their genes and express many common virulence factors (23), the disease they cause in immunocompetent humans is very different. One possible reason, expected to contribute to their different pathogenicity is a distinct expression of genes involved in host-pathogen interactions. To test this hypothesis, we compared the transcriptomic architecture and gene activity of SPA or STM in a disease-relevant context of epithelial cell infection. We chose to sample *Salmonella* infection at 8 h p.i. when the pathogen is considered to be well engaged in replication and optimally adapted to the intracellular environment (24). Thus, HeLa cells were infected with fluorescent STM and SPA for 8 h and sorted by flow cytometry to isolate *Salmonella*-infected cells. Isolated RNA was deep-sequenced (RNA-Seq), aligned to the corresponding *Salmonella* genome and compared to the transcriptome of *Salmonella* cultures growing extracellularly in rich LB medium.

RNA extracted from three independent infection experiments of HeLa cells infected with STM have generated 496-575 million RNA-Seq reads (human and bacterial reads) per experiment. Of which, 4.9-

6.6 million sequence reads, assigned to non-rRNA bacterial genes were used for intracellular bacterial transcriptome analysis. Three independent extracellular STM cultures grown in LB, were used as a reference control, from which we obtained 4.3-13.8 million RNA-seq informative reads that were assigned to non-rRNA bacterial genes. To analyze the STM gene expression, we calculated for each gene the number of transcripts per kilobase million (TPM) from its feature read count counts. The expression level threshold was set to a TPM value of 10 or above (25). Altogether, we identified 1,018 distinct genes that were exclusively expressed by STM during intracellular infection of HeLa cells and 191 distinct genes that were expressed only when STM was grown in LB. 3,127 transcripts were commonly expressed at both conditions (Fig. 1A and Table S1).

RNA-seq successfully identified 365 upregulated and 465 downregulated genes that were changed by at least twofold inside epithelial cells at 8 h p.i. (adjusted p-value ≤ 0.05) by STM, relative to their expression in LB (Fig. 2A and Table S2). In agreement with previous studies (14, 26, 27), during STM infection, at least 27 genes belonging to the flagella-motility regulon and several genes (*fimAWYZ*) from the type I fimbriae were significantly repressed. Interestingly, the expression of genes encoding the Saf fimbriae (*safABCD*) were upregulated during HeLa cell infections by STM.

In contrast to the flagella and the *fim* genes, at least 31 genes from the PhoPQ regulon were highly induced intracellularly (Fig. 2B). The two-component system PhoPQ, orchestrates *Salmonella* adaptation to the intracellular milieu and regulates a wide array of genes central for *Salmonella* virulence including those encoded on SPI-2 (28, 29). Correspondingly, we identified upregulation of the SPI-2 regulon including *ssaBCDEGHIJKLMVNOPRSTU*, *sseABCDEFGIJL*, *sseK3*, *sspH2*, *pipB, pipB2*, and *steC* genes (Fig. 2B). These results are consistent with the known notion that SPI-2 expression is induced during intracellular replication of *Salmonella* (15, 30) and with previous reports that studied STM expression during macrophages infection (31, 32). Other PhoP-regulated genes including *pgtE* (involved in bacterial

resistance to antimicrobial peptides), *pagN* (encoding an adhesion/invasion protein), *phoN* (acid phosphatase) and *pagCDJKO* were also induced (Fig. 2B).

Iron is an essential micronutrient required by nearly all bacterial species, including *Salmonella.* Limiting the availability of the nutrient metals to intracellular pathogens is one of the main mechanisms of nutritional immunity. In return, *Salmonella* uses a variety of high-affinity iron uptake systems to compete with the host for essential transition metals required for its intracellular growth (33). Indeed, we identified elevated expression of multiple iron (*entABEFH* and *iroNBCDE*), iron/ manganese (*sitABCD*), zinc (*zntR*, *zitT* and *znuA*), and magnesium (*mgtAB*) acquisition system genes, highlighting the essentiality of these metal ions for STM intracellular replication (Fig. 2B).

More than 100 suitable carbon substrates as well as various nitrogen, phosphorus and sulfur sources are available to invading pathogens, at different niches of the vertebrate hosts (34, 35). Interestingly, multiple genes belonging to the ethanolamine operon (*eutQTMGAC*) and genes involved in glycerol (*glpABDK*), and maltose (*malEKM*) metabolism were particularly induced during STM infection (Fig. 2B). Nevertheless, the most highly induced metabolic gene was *uhpT,* encoding a hexose phosphate transporter that was upregulated by more than 40-fold at 8 h p.i. These results suggest that sugar phosphates are major substrates required for cytosolic intracellular proliferation of STM within HeLa cells, but also that ethanolamine, glycerol and maltose could be utilized as alternative carbon sources in epithelial cells.

Similarly, biotin (*bioABCDF*), purine (*nrdEFHI* and *purDEHKLT*), and sulfate/thiosulfate (*cysACHITW* and *sufABCDES*) biosynthetic metabolic pathways were highly transcribed intracellularly by STM. Moreover, genes involved in biosynthesis of the amino acids histidine (*hisACDFH* and *hutG*), tryptophan (*trpABDE*), and glutamine (*glnAGKL*), and genes that catalyze the cleavage of N-acetylneuraminic acid

(sialic acid; Neu5Ac) to form pyruvate and N-acetylmannosamine (ManNAc) (*nanAEKT* and *nagB*) were also upregulated by STM during HeLa cell infections (Fig. 2B).

A large number of genes involved in phosphate metabolism were identified to be induced within HeLa cells. For example, the transcriptional levels of *pstABCS* (encoding an ATP-dependent phosphate uptake system), which is responsible for inorganic phosphate uptake during phosphate starvation, *ugpABCEQ, phoR* and *apeE* were markedly increased. The *ugp* operon is involved in hydrolysis of diesters during their transport at the cytoplasmic side of the inner membrane (36). Thereby, sn-glycerol-3-phosphate (G3P) is generated and used as a phosphate source. The *upg* operon is regulated by a two-component system, PhoBR, which also regulates the outer membrane esterase, ApeE (37). Additional genes belonging to the PhoB regulon, such as *phnSVWU* encoding the phosphonatase pathway, which is responsible for breaking down phosphonate and yielding cellular phosphate (38) were also significantly induced.

Collectively, these results suggest that STM likely experiences iron, biotin, purine and phosphate deprivation in host epithelial cells and induces the expression of genes involved in their transport and utilization. In addition, these results imply that ethanolamine, glycerol and maltose are available sources of carbon for STM in epithelial cells.

The intracellular transcriptomic landscape of *S*. Paratyphi A

RNA-Seq analysis was similarly applied for intracellular SPA. 313.8 to 805.9 million dual-RNASeq reads were obtained from three independent HeLa cell cultures infected with SPA. Out of these, 14.6 to 36.6 million sequence reads were assigned to non-rRNA SPA genes and used to determine the intracellular SPA transcriptome (Table S3). As a reference control, RNA extracted from SPA grown in LB from three independent cultures generated 7.3 to 23 million informative reads (assigned to non rRNA SPA genes). Overall, we identified 322 genes that were exclusively expressed (TPM ≥10) by SPA during

infection of HeLa cells compared to 576 genes that were expressed only by extracellular SPA in LB culture. 2,995 SPA genes were expressed at both conditions (Fig. 1B and Table S3).

At 8 h p.i. of HeLa cells, 322 genes were upregulated and 579 genes were down-regulated (Fig. 3A and Table S4) by twofold or more (adjusted p-value ≤ 0.05). Like in intracellular STM, the genes for type I (Fim) fimbriae (*fimCIWYZ*) and additional fimbria clusters including Bcf (*bcfDE*), the Curli (*csgBCDE*), Stb (*stbBE*), Stc (*stcABC*), Stf (*stfAD*), Sth (*sthABCD*), and Stk (*stkABC*) were all strongly downregulated intracellularly (Fig. 3B). Noteworthy, the downregulation of type I (*fimACIZ*), Curli (*csgBDE*) and Bcf (STM14_0037 and *bcfB*) fimbriae was more pronounced in SPA than in STM (Fig. S1), indicating that the SPA fimbriome is robustly repressed, during intracellular replication, while some basal level of expression of these fimbrial genes is still maintained during STM infection.

In contrast, but consistent with our findings for intracellular STM, genes belonging to the PhoPQ (including polymyxins resistance) and SPI-2 regulons were significantly induced by intracellular SPA. Moreover, various transition metals import systems including manganese and iron transporter (*sitABCD*), enterobactin biosynthesis system (*entABCDEF* and *fepAG*) and the iron ABC transporter IroC were considerably upregulated during SPA HeLa cell infection (Fig. 3B).

In addition, the expression of several metabolic pathways that were significantly elevated during STM infection were induced by intracellular SPA as well, including biotin (*bioABCDF*) and purine (*purCDEHKLT*) biosynthesis genes. Further overlap in the intracellular transcriptome of these pathogens includes several amino acid biosynthesis pathways such as glutamine (*glnAGKLPQ*), tryptophan (*trpABCDE*) and histidine (*hisAFGHI*) that were upregulated in both intracellular STM and SPA.

Nevertheless, comparison of the intracellular transcriptome between STM and SPA, during HeLa cells infection, identified 234 differentially expressed genes (DEGs; Table S5), indicating that some pathways may function differently during the intracellular phase of STM vs. SPA. These differences

included the induction of several amino acids biosynthesis genes which expression was more pronounced in intracellular SPA than in STM. These include biosynthesis genes of glycine (*glyASU*), isoleucine (*ilvCDEG*), leucine (*leuABCD*), lysine (*lysAC* and *sucBD*), methionine (*metCEFHKLR*), serine (*serAC*), and threonine (*thrBC*). In contrast, the threonine degradation pathway (*tdcABCDEG*) was found to be repressed in intracellular SPA. These results may suggest that SPA relies more than STM on amino acids as an available carbon and energy source during epithelial cell infection. Additional pathways that were found upregulated in SPA, but not in STM are the oxidative phosphorylation (*nuoEFGHIJKLMN* and *atpCD*), and peptidoglycan cell wall formation (*murACDEG*) pathway genes (Fig. 3B). Remarkably, further differences between the intracellular transcriptome of SPA vs. STM included different expression profiles of the SPI-1, motility and chemotaxis, and carbon utilization regulons as detailed in the following sections.

Differences in carbon catabolism during intracellular infection of *S*. Paratyphi A and *S*. Typhimurium

In order to survive, persist and replicate in host cells, intracellular pathogens must adapt their metabolic pathways to the specific physical conditions and available nutrients found in the intracellular environment. Carbon catabolism provides bacteria with energy by means of reducing equivalents, ATP and essential biosynthetic precursors. Different studies have suggested that hexose monosaccharides such as glucose and glucose-6P are the main source of carbon during *Salmonella* infection (39-43). Comparison of the metabolic gene expression between intracellular STM and SPA revealed significant differences in the expression profile of several carbon catabolic pathways. For example, the gene *uhpT* encoding an antiporter for external hexose 6-phosphate and internal inorganic phosphate (44) presented about 90-fold higher expression by intracellular STM than SPA (Fig. 4A). This different expression might be because the sensor-regulator system encoded by *uhpABC* is defective by pseudogene formation in SPA (45). Similarly, the gene coding for galactonate permeases (*dgoT*) was upregulated in intracellular

STM, but not in SPA, suggesting that STM utilizes more hexose 6-phosphate and galactonate than SPA as a carbon source during intracellular growth.

Similarly, RNA-Seq identified that at least seven genes involved in citrate metabolism including *citCDEFTX* and *citC2* exhibited higher transcription levels in intracellular STM than SPA (Fig. 4A). Independent qRT-PCR further confirmed that the intracellular expression of *citA* and *citX* encoding citrate-proton symporter and apo-citrate lyase phosphoribosyl-dephospho-CoA transferase, respectively is lower by about 3- and 10-fold in SPA infected cells vs. STM (Fig. 4B).

STM can utilize ethanolamine as a sole source of carbon, nitrogen, and energy in a cobalamin (vitamin B12)-dependent manner. Ethanolamine may be important to STM growth in the host, since it is derived from the membrane phospholipid phosphatidylethanolamine that is particularly prevalent in the gastrointestinal tract. This process involves breakdown of the precursor molecule phosphatidylethanolamine by phosphodiesterases to glycerol and ethanolamine (46). In STM, ethanolamine catabolism involves 17 genes organized in the *eut* operon, controlled by the transcriptional activator EutR (47). At least six ethanolamine catabolism genes (*eutSPQTGH*) were expressed at higher levels by intracellular STM compared to SPA (Fig. 4A). These differences were independently verified by qRT-PCR that showed significantly reduced expression of *eutG, eutP* and *eutQ* genes in intracellular SPA vs. STM (Fig. 4B).

Collectively, these observations suggest that STM is able to better utilize intracellular citrate, ethanolamine and galactonate as intracellular carbon sources than SPA, and that SPA may use an alternative carbon source such as amino acids during intracellular growth.

To further test this hypothesis, we compared the growth of SPA and STM in a defined M9 medium supplemented with ethanolamine or citrate as a carbon source. Growth under anaerobic conditions in M9 medium, supplemented with ethanolamine, without amino acids, did not allow bacterial growth of

neither STM nor SPA. Adding casamino acids, without additional carbon source, resulted in a minimal and comparable growth of both STM and SPA, likely due to the utilization of amino acids as a restricted carbon source. Nevertheless, adding ethanolamine as a *bona fide* carbon source to the medium resulted with increased and rapid growth of STM, but with a minor improvement of SPA growth (relative to its growth on amino acids only; Fig. 4C), indicating the ability of STM, but not SPA to efficiently ferment ethanolamine. Replacing the carbon source with citrate under aerobic growth conditions allowed delayed, but substantial growth of STM, in comparison to restricted and slower growth of SPA (Fig. 4D). These results are concurring with the expression data and indicate a better ability of STM than SPA to utilize both ethanolamine and citrate as a sole carbon source. These differences may also contribute to a higher intracellular replication pace of STM than SPA found in HeLa cells (Fig. S2).

Intracellular *S*. Paratyphi A expresses SPI-1 genes at higher levels than intracellular *S*. Typhimurium

Previously we showed that under extracellular aerobic growth conditions in LB, SPI-1 gene expression, as well as secretion of SPI-1-T3SS effector proteins, occur at significantly lower levels in SPA compared to STM (20). Here, in sharp contrast, we found that intracellular SPA transcribed significantly higher levels of SPI-1 and T3SS-1-effector genes than intracellular STM (Fig. 5A). This was clearly evident (log 2 change ≥ 2 and p-value ≤ 0.05) for at least 14 SPI-1 genes including the SPI-1 regulators *hilA* and *hilD*, the effector genes *sopBDF*, the T3SS-1 structural genes *invCHIJ* and *spaOPQ*, *sigE* encoding a chaperon (a.k.a. *pipC*) and *iagB* (Table S5).

Independent qRT-PCR was used to verify these observations and demonstrated that intracellular SPA transcribed *hilA*, *hilD*, *invH*, *sopB*, *sopD* and *spaO* at 4- to 27-fold higher levels than STM (Fig. 5B). Moreover, Western blotting against a 2HA-tagged version of SopB and SopE2 further indicated elevated

translation of these two SPI-1 effectors in intracellular SPA vs. STM (Fig. 5C). Collectively these results indicate that SPA expresses SPI-1 genes at higher levels during infection of non-phagocytic cells, in comparison to intracellular STM.

Intracellular *S*. Paratyphi A is motile and expresses flagella-chemotaxis genes at higher levels than *S*. Typhimurium

Functional flagella are necessary for *Salmonella* motility and invasion of host cells (21, 48, 49). In *S. enterica,* more than 50 genes are involved in the assembly and motion of flagella, organized in one regulon that composes three ordered regulatory phases corresponding to classes I (early), II (middle), and III (late) (50).

Previous studies have shown that the genes coding the flagellar machinery, as well as many genes involved in chemotaxis, are strongly repressed during STM intracellular lifestyle (27, 31, 32). Here, RNA-Seq analysis has demonstrated that at least 38 out of 50 chemotaxis and flagella genes, belonging to class II and III of the flagella regulon are expressed at significantly higher levels in intracellular SPA compared to STM (Fig. 6A and Table S5). These include the flagellin gene *fliC* that was expressed at 11-fold higher levels by SPA vs. STM, and many other flagellar genes including *flgC* that demonstrated 64-fold difference in its expression between intracellular SPA vs. STM. In addition to the flagellar genes, SPA residing in the host cell presented much higher expression levels of chemotaxis genes (e.g. *cheB, cheR, cheM, cheW, cheZ*, and *cheY*) than intracellular STM.

Independent qRT-PCR analysis confirmed these results and showed that in sorted infected HeLa cells, the expression of *fliC, fliZ, flgM, flgF, cheA* or *cheB* was 8- to 130-fold higher in intracellular SPA than in intracellular STM (Fig. 6B). In agreement with the RNA-seq and qRT-PCR analyses, Western

blotting using anti-FliC antibodies demonstrated significantly higher translation of FliC in intracellular SPA vs. STM (Fig. 6C). Taken together, these findings uncover significantly higher expression levels of motility and chemotaxis genes by SPA vs. STM within infected HeLa cells.

To further analyze if the increased expression of motility genes by intracellular SPA has physiological consequences, we investigated the possible presence of flagella in intracellular SPA. Immunostaining of intracellular SPA at 8 h p.i. indeed indicated the presence of flagella filaments on intracellular SPA (Fig. S3). Flagella staining was absent for a Δ*fliC* strain of SPA, and restored in the plasmid-complemented SPA Δ*fliC*. No immunolabeling of flagella was observed for intracellular STM WT or STM Δ*fliC* Δ*fljB* (Fig. S3).

Motile intracellular SPA are more inclined to replicate in the cytoplasm rather than the SCV

Analysis of host cells infected by STM or SPA WT or T3SS-2-deficient strains was performed. To distinguish *Salmonella* in the SCV from *Salmonella* in other compartments or in the cytosol, and to enable live-cell imaging of infected host cells, we used LAMP1-GFP expressing HeLa host cells (Fig. 7, Movies 1, 4). Lifeact-GFP expressing HeLa cells were used to investigate potential interactions with the host cell actin cytoskeleton (Movie 1-3).

More than 80% of STM WT were present in SCV with associated *Salmonella*-induced filaments (SIFs; Fig. 7A, Fig.8). STM WT was observed residing in SCV and the majority of infected host cells showed formation of extensive SIF networks. The STM *ssaV* strain was typically present in SCV, but tubular endosomal filaments were almost absent. A smaller proportion of host cells (ca. 10%) harbored cytosolic STM, and for these cells, massive cytosolic proliferation or hyper-replication was evident (Fig. 7A). For intracellular SPA WT, more heterogeneous phenotypes were observed (Fig. 7BCDE). SPA was located residing in the SCV, or present in the cytosol without association with LAMP1-positive membranes.

Intracellular SPA also induced SIF in a T3SS-2-dependent manner, but the frequency of SIF-positive cells was much lower with ca. 9% for SPA WT compared to more than 80% for STM WT (Fig. 7BC, Fig. 8). SPA-infected host cells often contained thin SIF, that are likely composed of single-membrane tubules, in contrast to SIF with more intense LAMP1-GFP signal, indicating double-membrane tubules (Fig. 7BC). For SPA WT, SIF formation was significantly less frequent, yet dependent on T3SS-2. The frequency of SPA associated with SCV marker LAMP1 was highly reduced compared to STM. As intracellular SPA was observed to reside in tightly enclosing SCV (51), we considered flagella expression by vacuolar SPA less likely than by cytosolic bacteria. Because transcriptional analyses showed expression of flagellar genes by intracellular SPA, flagella filaments were detected on intracellular SPA, and a major proportion of infected HeLa cells (~ 40%) harbored cytosolic SPA, we investigated the functional consequences of flagella expression by live-cell imaging of *Salmonella*-infected host cells (Movies 1-4). Indeed, we observed actively motile intracellular SPA in about 40% of the infection host cells.

As motility in intracellular microbes typically is mediated by polymerization of host cell actin by microbial surface proteins (52), we investigated F-actin dynamics in SPA-infected HeLa Lifeact-GFP cells (Movie 1). No association of F-actin with static or motile intracellular SPA was evident, and F-actin trails as observed for intracellular motile *Listeria monocytogenes* (53) were absent in SPA WT infected cells. No cytosolic motility was observed for intracellular STM. To control if cytosolic motility is linked to the observed flagella expression, we used a SPA *fliC* mutant strain. This non-motile mutant completely lacked cytosolic motility, but showed increased presence in SCV (Fig. 8, Movie 1). Cytosolic motility of SPA was not affected in the T3SS-deficient Δ*ssaR* strain (Fig. 8, Movie 1). Live-cell imaging at high frame rates (Movies 2 and 3) demonstrated the dynamics of intracellular motility of SPA in real time, with characteristic alternations between straight swimming and stops with tumbling. Analyses of the vectors

of individual SPA indicated collisions with the host cell plasma membrane, but there were no indications for formations of protrusions as observed for intracellular motile *L. monocytogenes* (53).

We next set out to analyze the broader relevance of intracellular motility of SPA and investigated a set of clinical SPA isolates (22), and SPA reference strains of SARB collection (54). We observed that all SPA strains tested showed intracellular motility in HeLa cells (Movie 4). Expression of flagella genes and presence of flagella filaments was previously demonstrated for STM in dead host cells extruded from polarized epithelial monolayers (55). As these experiments were performed with STM strain SL1344, we also analyzed this strain in our experimental setting. As for STM ATCC 14028, also STM SL1344 showed cytosolic hyper-replication in infected HeLa cells, but cytosolic motility was absent (Movie 4).

These data confirm that the expression of flagella by intracellular SPA leads to flagella-mediated cytosolic motility, and that this motility is a conserved trait specific to SPA.

Intracellular SPA are primed for reinfection of host cells

We set out to investigate potential functional consequences of the increased expression of SPI-1 and motility genes by intracellular SPA. We hypothesized that increased expression of SPI-1, higher amounts of T3SS-1 effector proteins, and motility could affect the interaction of SPA released from infected cells with naïve host cells. As host cell decay and release of the intracellular *Salmonella* is asynchronous, and quantification of new infection events is difficult in gentamicin protection assays, we set up a re-invasion assay that provides experimental control. HeLa cells were infected by invasive *Salmonella*, at a defined time point of 8 h p.i., host cells were osmotically lysed, and released bacteria were used to reinfect new epithelial cells. The number of viable bacteria in inoculum, released from initially infected host cells, and the number of bacteria in the second round of invasion were quantified (Fig. 9A).

We determined similar levels of invasion by SPA after microaerobic culture and STM after aerobic subculture (3.25% and 3.41% of inoculum, respectively), while STM after microaerobic subculture invaded less efficiently (0.47%). Interestingly, 6.88% of the SPA released from HeLa cells at 8 h p.i. were capable of reinvasion of naïve HeLa cells. In contrast, only 0.91% of released STM were able to reinvade, and reinvasion of STM after microaerobic culture was lower with 0.75%. These data indicate that higher expression of SPI-1 genes and bacterial motility by intracellular SPA results in increased invasiveness of SPA following exit from host cells (Fig. 9B).

DISCUSSION

Despite high genetic similarity, typhoid and non-typhoidal *Salmonella* serovars differ hugely in their host specificity, the immune response they elicit in humans, and the clinical manifestations they cause (56). Previously, we showed differences in host cell invasion and SPI-1 expression between STM and SPA, following extracellular growth in rich medium LB under aerobic conditions (20) and demonstrated that elevated physiological temperature affects differently their motility and host cell entry (22, 51).

In this work, we focused on their intracellular phase of infection and have taken an unbiased deep RNA-Seq approach to get a panoramic view of the intracellular STM and SPA transcriptomic architecture, and to identify differences in the activity of their genes in the intracellular milieu. Following transition from extracellular to the intravacuolar environment, *Salmonella* undergoes extensive adaptation and global modulation of gene expression to respond to the intracellular environment, however the nutritional contents of the SCV and the metabolic pathways required during intracellular growth are largely undefined. Amino acids and purines seem to be deficient since previous studies have shown that many auxotrophic *Salmonella* mutants are unable to grow intracellularly and are severely attenuated for

396 virulence in mice (57-60). These observations suggest that intracellular *Salmonella* depend on *de novo*
397 synthesis of metabolic precursors.

398 Recently, Liu and colleagues have applied a proteomic approach to determine the expression of
399 STM proteins within HeLa cells at 6 (61) and 18 h (27) p.i. Also, the STM transcriptome inside
400 macrophages (31, 32) and epithelial cells (26) has been reported previously. Nevertheless, a global
401 transcriptomic comparison between SPA and STM during intracellular infection has not been published
402 thus far.

403 Previous efforts to identify changes in gene expression using quantitative proteomic approach (LC-
404 MS/MS analyses) have revealed that among about 3,000 detected proteins, the expression of 100
405 *Salmonella* proteins significantly changed (61 were upregulated and 39 proteins were downregulated)
406 during the transition of STM from the extracellular to the intracellular niche of HeLa cells, at 6 h p.i. (61).
407 A microarray hybridization-based technique has identified 605 upregulated and 616 downregulated STM
408 genes at 6 h p.i. of HeLa cells (26). Our current transcriptomic analysis identified 830 differentially
409 expressed STM genes (365 upregulated and 465 downregulated) that were altered at 8 h p.i., relative to
410 their extracellular expression. Similar numbers of DEGs were also detected for SPA, which presented 322
411 upregulated and 579 downregulated genes, during epithelial cell infection.

412 In agreement with these previous analyses, we observed substantial downregulation in the
413 expression of genes associated with SPI-1, Type I fimbriae, flagella and chemotaxis systems in STM, but
414 significant upregulation of STM genes involved in metal ions uptake, purines and biotin synthesis. In fact,
415 nearly all known *Salmonella* iron-, zinc-, or manganese-responsive pathways were found to be
416 intracellularly induced. Since the SCV is characterized by low levels of magnesium, manganese, iron and
417 zinc metals (62) and given the pivotal role of these metal ions in *Salmonella* infection (63, 64),
418 upregulation of iron, zinc and manganese acquisition system genes is not surprising. Nonetheless, these

results highlight the importance of biotin and purines to the intracellular phase of *Salmonella* during infection. This notion is consistent with (i) SCVs of both macrophage and epithelial cells are limited for purines and pyrimidines (65); (ii) the avirulent phenotype of purine auxotrophic mutants of *S*. Typhimurium and *S*. Dublin in mice (59); and (iii) the reported contribution of biotin sulfoxide reductase to oxidative stress tolerance and virulence of *Salmonella* in mice (66).

Interestingly, in contrast to the proteomics (61) and the microarray-based transcriptome analyses (26), we were also able to identify significant upregulation of SPI-2 and PhoPQ regulon genes both in STM and SPA. These differences may reflect the time point differences (8 h p.i. in our analysis vs. 6 h p.i. in previous analyses), or the superior sensitivity of the current RNA-Seq techniques.

While the change in the expression of metal transport systems, purines, biotin, PhoPQ and SPI-2 regulons was common to both SPA and STM, intriguing differences in the expression profile of SPI-1, motility and chemotaxis, and carbon utilization pathways (mainly citrate, galactonate and ethanolamine) were identified between intracellular SPA and STM. Ethanolamine is a ubiquitous molecule within vertebrate hosts and serves as a carbon and nitrogen source for bacteria in the intestine, as well as within epithelial cells (67). *Salmonella* can utilize ethanolamine, as an exclusive source of carbon and nitrogen, generating acetaldehyde and ammonia. The ammonia can then provide a cellular supply of reduced nitrogen, while the acetaldehyde can be converted into the metabolically useful compound acetyl-CoA (68). Our data indicated much higher expression of multiple ethanolamine utilization genes by STM vs. SPA during host cell infection and more efficient utilization *in-vitro*. Recently, it was shown that ethanolamine metabolism in the intestine enables STM to establish infection and that EutR, the transcription factor of the ethanolamine cluster in *Salmonella* directly activates the expression of SPI-2 in the intracellular environment (69, 70).

The sugar acid galactonate is another example of an available carbon and energy source that is produced in the mammalian gut. The gut microbiota releases sugar acids including galactonate from ingested polysaccharides present in nutrients by the host, or from simple sugars as catabolic intermediates of metabolism (71). These results may suggest that STM utilizes galactonate, citrate and ethanolamine more effectively than SPA as available carbon sources, and that STM may better coordinate ethanolamine metabolism and virulence via EutR during infection. This notion is consistent with our *in-vitro* data showing that while STM is able to utilize ethanolamine and citrate as a sole carbon source, SPA cannot grow or grows much slower on these sources. Previous studies have shown that deficiency for citrate lyase activity (*citF*) leads to significant reduction in STM survival inside macrophages (72) and that an STM mutant that cannot utilize citrate is highly attenuated in the mouse (73). Similarly, ethanolamine is released by host tissues during inflammation and a study by Thiennimitr and colleagues in mice has shown that ethanolamine metabolism provides a growth advantage to STM during intestinal colonization (70). Since SPA provokes a noninflammatory disease, it is possible that SPA has lost the ability to utilize ethanolamine as it provides no advantage during noninflammatory infection.

It is well established that the expression of the flagella and chemotaxis are highly repressed by intracellular STM (27, 31, 61, 74), supporting a nonmotile state of intracellular STM. In agreement with these reports, we have also observed extensive repression of the entire motility-chemotaxis regulon in intracellular STM, however we found significantly higher expression of this regulon in intracellular SPA. Similar observations were also obtained for the evolutionary related T3SS-1 genes. Most salmonellae are motile and express peritrichous flagella around its membrane. Like T3SS-1, *Salmonella* motility is playing an important role in host colonization and virulence (75, 76). Previous reports have shown a regulatory association between T3SS-1 and the flagella in STM (77). Subsequent to STM entry into host cells, the intracellular expression of T3SS-1 (27, 31, 78) as well as flagella production and chemotaxis (27, 31, 61, 79) genes were shown to be highly repressed, possibly to prevent inflammatory response by the

NAIP/NLRC4 inflammasome (80). Therefore, it was unexpected to find that the flagella regulon is readily expressed during SPA intracellular infection and that it maintains an intracellular motility during epithelial cell infection.

Intracellular motility is long known in bacterial pathogens such as *Listeria monocytogenes, Shigella flexneri*, *Rickettsia* spp., and *Burkholderia* spp., that all exhibit intracellular actin-based motility to spread from cell to cell (81). Nonetheless, to the best of our knowledge, this is the first report of a flagellum-dependent intracellular motility of any *Salmonella* serovar in living host cells. While we did not find evidence for intercellular spread, it is possible that this mechanism facilitates escape of SPA from the SCV to the cytoplasm. Previous studies have shown that a small subpopulation of hyper-replicating STM resides within the cytosol of epithelial cells and serves as a reservoir for dissemination. These motile bacteria retain both SPI-1 and flagella expression, but present a low expression of SPI-2 genes, and therefore are primed for invasion (82). This expression profile is largely similar to the intracellular profile of SPA. Indeed, we showed that intracellular SPA possesses higher ability to reinfect non-phagocytic cells than intracellular STM. We propose that elevated expression of motility-chemotaxis and SPI-1 genes in addition to flagella-mediated motility prime SPA towards a new cycle of host cell infection, supporting systemic dissemination of this pathogen in the human body. These phenotypes may contribute to the invasive nature of paratyphoid fever and the ability of SPA to disseminate beyond the intestinal lamina propria of the human host. Future work has to reveal which cells or tissues of infected host organisms are affected by intracellular motility of SPA. However, such analyses are hampered by the lack of animal models for infection. Infection models with human organoids (83), for examples based on gall bladder epithelial organoids (84) as a tissue type important for SPA persistence and dissemination, may offer new perspectives for analyses of cellular interactions.

MATERIAL AND METHODS

Bacterial strains, growth conditions and data sets. Bacterial strains utilized in this study are listed in **Table S6** . *S*. Typhimurium 14028 S (85) and *S*. Paratyphi A strain 45157, an epidemic strain, responsible for a paratyphoid outbreak in Nepal (9) were used as the wild-type strains. Bacterial cultures were routinely maintained in Luria-Bertani (LB; BD Difco) liquid medium at 37°C. An M9 medium [33.7 mM Na_2HPO_4, 22 mM KH_2PO_4, 8.5 mM NaCl, 18.7 mM NH_4Cl, 12.1% Trizma base, pH=7.4] supplemented with 2 mM $MgSO_4$, 0.3 mM $CaCl_2$, 3.7 µM thiamine, 4.1 µM biotin, 0.134 mM EDTA, 31 µM $FeCl_3$, 6.2 µM $ZnCl_2$, 7.6 nM $CuCl_2$, 4.2 nM $CoCl_2$, 1.62 µM H_3BO_3, 8.1 nM $MnCl_2$, with or without 0.1% Casamino acids, and with one of the following carbon sources glucose (11 mM), ethanolamine hydrochloride (51 mM) or sodium citrate (34 mM) was used as a minimal growth medium.

For HeLa cell infections, *Salmonella* cultures were grown to the stationary phase under microaerobic conditions (see below). The final dataset for RNA-seq included 12 samples resulting from three independent growth in LB or infection experiments that were used for RNA extraction: (i) *S*. Typhimurium 14028 S bacterium grown in LB medium (hereafter named STM_m) (ii) *S*. Paratyphi A strain 45157 grown in LB medium (hereafter named SPA_m) (iii) Typhimurium 14028 S bacterium infected Hela-cells (hereafter named STM_i) and (iv) *S*. Paratyphi A strain 45157 bacterium in Hela-cells (hereafter named SPA_i).

Infection of HeLa cells. Human epithelial HeLa (ATCC CCL-2) cells were purchased from the American Type Culture Collection and were cultured in a high-glucose (4.5 g/l) DMEM supplemented with 10% FBS, 1 mM pyruvate and 2 mM L-glutamine at 37 °C in a humidified atmosphere with 5% CO_2. Cells were seeded at 6×10^6 cells/ml in a onewell plate (Greiner) tissue culture dish 18 h prior to bacterial infection and infected at multiplicity of infection (MOI) of ~200 (bacteria per cell). For RNA extraction, five plates for *S.* Typhimurium and six plates for *S.* Paratyphi A were used. *Salmonella* strains carrying the

pBR-GFP2 plasmid were grown in 2 ml LB containing 20 µg/ml tetracycline at 37 ˚C with shaking (250 rpm) for 6-8 h, and then diluted 1:75 into 10 ml LB supplemented with 20 µg/ml tetracycline and grown without shaking at 37 ˚C for 16 h. Bacterial cultures were centrifuged for 5 min at 4,629 × g, at room temperature (RT), and resuspended in 3 ml prewarmed complete DMEM. 3 ml of DMEM suspended Salmonellae (~2.5×10^9 CFU) were used to replace the medium of seeded cells and plates were centrifuged for 5 minutes at 142 × g at RT. After centrifugation, 7 ml of prewarmed DMEM were added and plates were incubated at 37 ˚C under 5% CO_2 atmosphere. At 2 h post infection (p.i.) the medium was aspirated, cells were washed three times with 10 ml PBS containing $CaCl_2$ and $MgCl_2$ (PBS +/+), and incubated with 10 ml prewarmed DMEM containing 100 µg/ml gentamicin. After 60 min, the media was replaced with DMEM containing 10 µg/ml gentamicin and cells were further incubated as before. At 8 h p.i., the cells were washed three times with 10 ml PBS +/+ and trypsinized with 2 ml prewarmed trypsin at 37 ˚C. When the cells were detached, prewarmed DMEM was added to quench the trypsin. The cells were transferred to a 50 ml conical tube, precipitated by 5 min centrifugation at 247 x g and washed in 15 ml PBS+/+. Finally, the cells were resuspended in 1 ml / plate fixation reagent (RNAlater: RNAprotect 350:1), incubated at RT for 20 min, and then stored at 4 °C until sorting.

HeLa cell lines stably transfected for expression of LAMP1-GFP or Lifeact-GFP have been described before (86) and were maintained and infected as described above.

FACS sorting and RNA extraction. RNA was extracted from three independent infection experiments of HeLa cells with STM strain ATCC 14028S or SPA 45157. As controls, RNA was also extracted from three independent cultures of uninfected cells and from bacterial cultures grown in LB. HeLa cells (infected or uninfected) were fixed, centrifuged at 247 × g for 5 min and resuspended in 3 ml PBS+/+. The cells were filtered through 30 µm pre-separation filter into 5 ml FACS tubes (SARSTEDT) and sorted on a BD-FACSAria IIu (100 µm nozzle; ND filter 2) at a rate of approximately 300 cells/sec. 2-

535 2.5×10^6 GFP-positive (infected) HeLa cells were collected and centrifuged at 247 × g for 5 min. RNA
536 extraction was performed using Hybrid-R RNA Purification System (GeneAll). RNA samples were treated
537 with RNase-free DNase (Qiagen) according to manufacturer's protocol, followed by ethanol precipitation
538 and Ribosomal RNA depletion that was performed by Epidemiology Ribo-Zero Gold rRNA Removal Kit
539 (Illumina).

540 **RNA sequencing.** RNAseq was performed at the GeT-PlaGe core facility, INRAE Toulouse. RNA-
541 seq libraries were prepared using the Illumina TruSeq Stranded mRNA Library Prep, without a poly-A
542 mRNA selection, according to the manufacturer's protocol. Briefly, RNAs were fragmented to generate
543 double-stranded cDNA and adaptors were ligated. 11 cycles of PCR were applied to amplify the libraries
544 and their quality was assessed using a Fragment Analyser. Libraries were quantified by qPCR using the
545 Kapa Library Quantification Kit (Roche). To reach 5 million bacterial reads for each sample, as
546 recommended in (87), RNA-seq reads were generated from three lanes of an Illumina HiSeq3000 and
547 two lanes of an Illumina NOVAseq6000 using a paired-end read length of 2×150 bp. Ribosomal RNA
548 (rRNA) reads were filtered out using sortmerna-2.1b (88) against Silva and Rfam databases. The raw reads
549 data for this study have been deposited in the European Nucleotide Archive (ENA) at EMBL-EBI
550 under accession number PRJEB46495 and as specified in Table S7.

551 **Genome annotation and quality control.** A flowchart summarizing the RNA-seq pipeline and
552 bioinformatic analyses is shown in Fig. S4. Annotation of SPA 45157 and STM 14028S genomes was
553 performed using EugenePP 1.2 (89) with general and targeted evidence to predict coding genes and
554 noncoding features (Figure S1). Functional prediction was produced with InterProscan v5.15-54.0 with
555 GO terms, COG version COG2014 (90), REBASE v708 (91), IslandViewer4 (92) and PHAST (93).

556 Structural and regulatory non-coding RNA were annotated using RNAspace software v1.2.1 (94)
557 together with the following tools: RNAmmer 1.2 for rRNA (95), tRNAScan-SE 1.23 for tRNA (96) and blastn

2.2.25 against RFAM 10.0 for other ncRNA (97). The gff3 files produced by Eugene and RNA annotation were merged by a semi-manually procedure using BEDTools-2.26.0 (98).

FastQC v0.11.7 was used for quality control of the raw sequence data. Cutadapt 1.8.3 was used to remove Illumina Truseq adaptors and to filter out all reads with length shorter than 36 nucleotides.

Reads mapping and counting. The remaining, non rRNA reads were mapped with STAR-2.6.0c (99), with default parameters, against a "hybrid" genome composed by the Ensembl GRCh38 human primary assembly (release 92) and the SPA (accession number CP076727) or STM (accession number CP001362 - CP001363) genomes. In addition, in order to analyze bacterial samples, we indexed each bacterial genome separately by decreasing the parameter "genomeSAindexNbases" to 10 for STM and to 9 for SPA, while producing the alignment (.bam) files sorted by coordinates. Samtools flagstat v1.8 was used to obtain mapping statistics. Then we added read groups to trace the origin of each read with AddOrReplaceReadGroups of Picard tools v2.18.2. Next, we merged the bam files that originated from resequencing of the same sample using the MergeSamFiles command of Picard tools. The featureCounts command from the Subread-1.6.0 tool (100) was used to compute fractional counting for all annotated genes.

Clustering of orthologous genes. Orthologous genes were computed using Roary v.3.11.2 (101) with default parameters (minimum of 95% identity between coding sequences of the same cluster) except for the "-s" option that avoids paralog splitting in different clusters. Based on the orthologous groups, we produced raw count matrices that compare the expression level between orthologous genes of SPA and STM. We also added groups including paralog genes on either SPA or STM genome into the raw count matrix to sum up the raw reads count of each putative paralog gene.

Differential Gene expression analysis. Normalization and differential analysis were carried out according to the DESeq2 model and package (102) using adjusted p-value with FDR correction and the

Wald test to infer the probability value. Genes that had too few reads (the sum of reads for all the samples was less than 10) were discarded. To compare DEGs between SPA and STM, we created a count matrix composed of the shared protein-coding and ncRNA genes between these two serovars. The heatmaps were created by applying DESeq2 variance stabilizing transformations (the vst command) on the counts followed by subtracting the mean of the gene across all samples. The heatmaps were drawn using the ComplexHeatmap R package (103).

Reverse transcription and quantitative real-time PCR (qRT-PCR). 500 ng of RNA was reverse-transcribed using qScript cDNA synthesis kit (Quanta-bio). Real-time PCR was performed as previously described (20) on a StepOnePlus Real-Time PCR System (Applied Biosystems). Relative quantity of transcripts was calculated as $2^{-\Delta\Delta Ct}$, using the *rpoD* gene as an endogenous normalization control.

Western Blotting. HeLa cells were infected with *Salmonella* strains carrying pBR-GFP2 plasmid and pWSK29 carrying HA-tagged alleles of *sopE2* and *sopB*. The infection procedure was performed as above until the fixation step. Cell fixation was performed by incubation with 5 ml of 4% formaldehyde for 15 min under gentle shaking. Five ml of PBS +/+ were added and the cells were centrifuged for 5 min at 2,700 × g. Subsequently, the cells were washed three times with PBS +/+ and finally resuspended in PBS +/+ containing 1% BSA. The cells were stored at 4 °C until sorting. 1×10^6 GFP-positive cells were centrifuged for 5 min at 247 × g, and resuspended in 100 µl sample buffer. Western blot of the infected cells was performed as previously described (104) using the anti-2HA (Abcam ab18181; 1:1,000), anti-FliC (Abcam ab93713; 1:200,000) and anti-DnaK (Abcam ab69617; 1:10,000). Proteins were quantified relative to DnaK using ImageJ.

Host cell infection and live-cell imaging. HeLa cells stably transfected with LAMP1-GFP were seeded in surface-treated 8-well slides (ibidi) 24 or 48 h prior to infection to reach ~80% confluency (~80,000 cells) and were then used for infection. STM strains for infection experiments were subcultured

from an overnight culture (1:31) in fresh LB medium and grown for 3.5 h at 37°C. For infection, SPA strains were grown for 8 h under aerobic conditions, subcultured (1:100) in fresh LB medium and stationary-phase subcultures were grown for 16 h under microaerophilic conditions as described in (21). Bacteria were adjusted to an optical density of 0.2 at 600 nm in PBS and used for infection with the respective MOI (between 25 and 100, dependent on strain). Bacteria were centrifuged onto the cells for 5 min at 500 × g to synchronize infection and the infection was allowed to proceed for 25 min. After washing thrice with PBS, cells were incubated in medium containing 100 µg × ml^{-1} of gentamicin to kill extracellular bacteria. Afterwards, the cells were maintained in medium supplemented with 10 µg × ml^{-1} gentamicin for the ongoing experiment. Live-cell imaging was performed with Cell Observer Spinning Disc microscope (Zeiss) equipped with a Yokogawa Spinning Disc Unit CSU-X1a5000, an incubation chamber, 63× objective (α-Plan-Apochromat, NA 1.4), two ORCA Flash 4.0 V3 cameras (Hamamatsu) and appropriate filters for the respective fluorescence proteins.

Immunostaining of infected cells. HeLa cells stably transfected with LAMP1-GFP were seeded in surface-treated 24-well plates (TPP) on coverslips 24 h or 48 h prior infection to reach ~80% confluency (~180,000 cells) and were used for infection. Cultivation of bacteria and infection of HeLa cells was carried out as described above. After the desired incubation time the cells were washed thrice with PBS and fixed with 3% PFA in PBS for 15 min at RT, followed by immunostaining. Fixed cells were washed thrice with PBS and incubated in blocking solution (2% goat serum, 2% bovine serum albumin, 0.1% saponin, 0.2 % Triton X-100) for 30 min. Cells were stained 1 h at RT with primary antibodies against *Salmonella* (H:i, BD Difco 228241; H:a, Sifin TR1401; O:5, Sifin TR5303). After washing thrice with PBS, cells were incubated with the appropriate secondary antibodies for 1 h at RT. Coverslips were mounted with Fluoroshield (Sigma) and sealed with Entellan (Merck). Microscopy of fixed samples was either performed using a Cell Observer Spinning Disc microscope (Zeiss) as described above, or using a Leica

SP5 confocal laser-scanning microscope using 100× objective (HCX PL APO CS, NA 1.4-0.7) and polychroic mirror TD 488/543/633.

Reinvasion assays. HeLa cells were seeded in surface-treated 6-well plates (TPP) 24 h or 48 h prior to infection to reach ~100% confluency (1×10^6 cells) on the day of infection. Infection cultures of STM and SPA strains were grown as either 3.5 h aerobic or 16 h microaerobic subcultures and used for infection as described above. At 1 h p.i., cells were washed thrice with PBS and lysed using 0.1% Triton X-100. CFU were determined by plating serial dilutions of lysates and inoculum on Mueller-Hinton II (MH) agar and incubated overnight at 37 °C. The percentage of internalized bacteria of the inoculum (from subcultures) was calculated. 8 h p.i., cells were washed twice with PBS, once with ice-cold ddH_2O, and lysed using ddH_2O. Bacteria liberated from host cells by hypotonic lysis were used to infect naïve HeLa cells, and 1 h p.i. cells were washed and lysed and CFU were determined as described above. The percentage of internalized bacteria of the inoculum (from liberated bacteria) was calculated.

ACKNOWLEDGMENTS

This work was supported by the Infect-Era program, SalHostTrop project ("Understanding the Human-Restricted Host Tropism of Typhoidal Salmonella", 2016-2020) and by the France Génomique National infrastructure, funded as part of "Investissement d'avenir" program managed by Agence Nationale pour la Recherche (ANR-10-INBS-09 contract). The work at the Gal-Mor laboratory was supported by grant numbers: 2616/18 from the joint ISF-Broad Institute program; 3-12435 from Infect-Era /Chief Scientist Ministry of Health; I-41-416.6-2018 from the German-Israeli Foundation for Scientific Research and Development (GIF, awarded to OGM and MH); and A128055 from the Research Cooperation Lower Saxony – Israel (The Volkswagen Foundation, awarded to OGM, MH and GG). The

649 funders had no role in study design, data collection, and interpretation, or the decision to submit the
650 work for publication. We thank C. Gaspin for providing annotation of ncRNA genes of the STM and SPA
651 genomes.

652

653 **FIGURE LEGENDS**

654 **Figure 1. The number of STM and SPA genes expressed in LB medium and during intracellular**
655 **growth.** *Salmonella* RNA-seq reads were aligned to *S*. Typhimurium 14028S and *S*. Paratyphi A 45157
656 genomes and normalized by transcripts per million (TPM) transformation. Genes with TPM ≥ 10 were
657 considered as expressed. The number of expressed genes in STM (**A**) and SPA (**B**) growing in LB medium
658 to the late logarithmic phase and within HeLa cells at 8 h p.i. is shown.

659 **Figure 2. DEGs of intracellular *S*. Typhimurium compared to growth in LB medium. (A)** Volcano
660 plots showing the fold change (log2 ratio) in the expression of STM genes grown intracellularly in HeLa
661 cells (8 h p.i.) vs. the growth in LB medium (X-axis) plotted against the -$\log_{10}$ adjusted p-value (Y-axis).
662 Each dot on the plot represents the mean value (from three independent cultures) of one gene. Genes
663 that were changed by more than twofold are colored in red. (**B**) Heatmap based on RNA-Seq results
664 showing the relative transcription of STM genes of interest during intracellular infection (C1 to C3) vs.
665 their extracellular expression in LB medium (M1 to M3).

666 **Figure 3. DEGs of intracellular *S*. Paratyphi A compared to growth in LB medium. (A)** Volcano
667 plots showing the fold change (log2 ratio) in the expression of SPA genes grown intracellularly in HeLa
668 cells (8 h p.i.) vs. the growth in LB medium (X-axis) plotted against the -$\log_{10}$ adjusted p-value (Y-axis).
669 Each dot on the plot represents the mean value (from three independent cultures) of one gene. Genes
670 that were changed by more than twofold are colored in red. (**B**) Heatmap based on RNA-Seq results
671 showing the relative transcription of SPA genes of interest during intracellular infection (C1 to C3) vs.
672 their extracellular expression in LB medium (M1 to M3).

673 **Figure 4. Differences in carbon utilization gene expression between STM and SPA.** (**A**) Heatmap
674 of carbon catabolism gene expression by intracellular STM vs. intracellular SPA. Pseudogenes in the SPA
675 genome are marked with an asterisk. (**B**) The fold change in the transcription of the glucose-6P (*uhpT*),

citrate (*citA* and *citX*), and ethanolamine (*eutP, eutQ* and *eutG*) utilization pathways in intracellular STM relative to their expression in intracellular SPA was determined using qRT-PCR. RNA was extracted from FACS-sorted intracellular salmonellae 8 h p.i. The mean and the standard error of the mean of 3-8 independent qRT-PCR reactions are shown. Student t-test was used to determine statistical significance. **, $p < 0.005$; ***, $p < 0.0001$; ND, not detected. (**C**) Growth of STM and SPA in M9 in the presence (+) or absence (-) of casamino acids (AA) and ethanolamine (ETA), under anaerobic conditions. (**D**) Growth of STM and SPA in M9 supplemented with citrate as a sole carbon source.

Figure 5. Intracellular SPA expresses higher levels of SPI-1 genes than intracellular STM. (**A**) Heat map of RNA-Seq results showing the relative transcription of SPI-1 genes in three independent HeLa cell infections with STM and SPA. (**B**) The fold change in the transcription of six SPI-1 genes (*hilA, hilD, invH, sopB, sopD* and *spaO*) in intracellular SPA relative to their expression in intracellular STM was determined by qRT-PCR. The results show the mean of 3-6 qRT-PCR reactions and the error bars indicate the SEM. (**C**) SPA and STM strains expressing GFP and a 2HA-tagged version of the SPI-1 effectors SopE2 and SopB were used to infect HeLa cells. At 8 h p.i., cells were fixed and FACS-sorted for infected (GFP-positive cells). Infected HeLa cells (1×10^6 for each sample) were collected and separated on 12% SDS-PAGE. Western blotting using anti-hemagglutinin (HA) tag antibodies was used to detect the intracellular expression of SopE2 and SopB. Anti-DnaK antibodies were used as a loading control.

Figure 6. Intracellular SPA expresses higher levels of motility-chemotaxis genes than intracellular STM. (**A**) Heat map of RNA-Seq results showing the relative transcription of the motility-chemotaxis regulon in three independent HeLa cells infections with STM and SPA. (**B**) The fold change in the transcription of six flagellum genes (*fliC, fliZ, glgM, flgF, cheA* and *cheB*) in intracellular SPA relative to their expression in intracellular STM was analyzed by qRT-PCR. The results show the mean of 3-5 independent reactions and the error bars indicate the SEM. (**C**) SPA and STM strains expressing GFP were

699 used to infect HeLa cells. At 8 h p.i., cells were fixed and FACS-sorted. Equal numbers of 1×10^6 infected
700 HeLa cells were collected, lysed, and proteins were separated on 12% SDS-PAGE. Western blotting using
701 anti-FliC antibodies were used to detect synthesis of FliC by intracellular *Salmonella*. Anti-DnaK
702 antibodies were used as a loading control.

703 **Figure 7. Distinct phenotypes of intracellular SPA.** HeLa cells stably transfected for expression of
704 LAMP1-GFP (green) were infected with STM WT (**A**, MOI 25) or SPA WT (**B-E**, MOI 75), each harboring
705 pFPV-mCherry for constitutive expression of mCherry (red). Live-cell imaging was performed at 8 h p.i.
706 Images are shown as maximum intensity projection. Arrowheads indicate subpopulations with distinct
707 phenotypes in infected cells: SIF (green), thin SIF (green with asterisk), *Salmonella* residing in SCV
708 (yellow), cytosolic *Salmonella* (red), hyper-replicating cytosolic *Salmonella* (red with asterisk). Scale bars:
709 10 µm (overview), 5 µm (inset).

710 **Figure 8. Quantification of intracellular phenotypes.** HeLa cells stably expressing LAMP1-GFP
711 (green) were infected with *Salmonella* strains expressing mCherry (red). Quantification of intracellular
712 phenotypes was performed with a Zeiss Cell Observer with 63x objective. From 6-8 h p.i. at least 100
713 infected cells per strain (for SPA *fliC* at least 50) were examined for intracellular phenotype. Data
714 represent the means with standard deviations for three biological replicates for each strain and
715 condition. Statistical analysis was performed with One-way ANOVA and is indicated as n.s., not
716 significant; *, $p < 0.05$; **, $p < 0.01$; ***, $p < 0.001$.

717 **Figure 9. SPA shows higher invasion after release out of infected cells. (A)** HeLa cells were infected
718 with STM WT or SPA WT at MOI 5, and invasion by each strain was determined by gentamicin protection
719 assays. At 8 h p.i., one portion of infected cells was lysed by hypotonic conditions, and the released
720 bacteria were used to reinfect naive HeLa cells. (**B**) Intracellular CFU counts were determined 1 h p.i.
721 after initial infection (invasion, black bars), or 1 h p.i. after infection with *Salmonella* released from host
722 cells at 8 h p.i. (reinvasion, grey bars). Depicted are means and SD of three biological replicates, each

723 performed in triplicate. For statistical analysis, Student's t-test was performed. Significance is indicated
724 as n.s., not significant; *, $p < 0.05$; **, $p < 0,01$; ***, $p < 0.001$.

725

726 **SUPPLEMENTARY MATERIALS**

727 **Fig. S1. Expression of fimbriae genes in intracellular STM vs. SPA.** (**A**) Heat map of RNA-Seq
728 results showing the relative transcription of genes encoding curli (Csg), Fim, or Bcf fimbriae in three
729 independent HeLa cells infections with STM and SPA. (**B**) The x-fold change in the expression of *csgA* and
730 *csgD* in intracellular SPA relative to their expression in intracellular STM was analyzed by qRT-PCR. The
731 results show the means of 4-8 independent reactions and the error bars indicate the SEM.

732 **Fig. S2. Intracellular replication of SPA and STM in HeLa cells.** Intracellular growth of STM vs. SPA
733 in HeLa cells at 2, 4, 6, 8 and 24 h p.i. Bacterial replication was determined by the gentamicin protection
734 assay. Replication was calculated as the ratio between the intracellular bacteria (CFU) recovered at each
735 time point and the number of CFU at 2 p.i. The means and the SEM of four independent infections are
736 shown.

737 **Fig. S3. Formation of flagella by SPA within the host cell cytoplasm.** HeLa cells stably expressing
738 LAMP1-GFP (green) were infected with SPA WT, SPA *fliC*, SPA *fliC* [*fliC*], STM WT, or STM *fliC fljB* as
739 indicated, each constitutively expressing mCherry (red). Infected cells were fixed 8 h p.i. and
740 subsequently immunolabeled with serovar-specific antibody against FliC (blue). Scale bars: 10 µm.

741 **Fig. S4. A flowchart of RNA-seq and bioinformatic analyses.** The different steps and main tools
742 used for the bioinformatic analyses illustrated. RNA extracted from STM and SPA grown in culture and
743 from infected cells was subjected to NGS on Illumina sequencing. RNA-seq reads were cleaned and
744 quality controlled using FastQC. Cutadapt was used to remove Illumina Truseq adaptors and to filter out
745 all reads shorter than 36 nucleotides. SortMeRNA was used to filter out ribosomal RNA reads from raw

data. Human and bacterial genomes were merged into "Hybrid genomes" and indexed with STAR. Bacterial genomes were reannotated using EugenePP. STAR was used to align reads to reference genomes and sort resulting bam files by coordinates. To compute fractional counting for all annotated coding and non-coding genes the Subread tool with parameters "-s 2 (reversely stranded), -p (count fragments instead of reads) -M, -O, --fraction" was used. Clustering of *Salmonella* homologous genes was computed using Roary. Normalization and differential expressed genes analysis were carried out according to the DESeq2 model and package using adjusted P-value and the Wald test to infer the probability value. To obtain DEGs between STM and SPA a count matrix composed of the shared and coding genes and ncRNAs between these two serovars was created.

TABLES

Table S1. The transcriptome of STM grown in LB and intracellularly. The RNA-seq reads obtained from STM grown on LB or extracted from HeLa cells infected with STM were mapped to the STM 12048S genome. This table shows the normalized (TPM) featurecount counts of reads assigned to the STM genes. This table also lists the genes that were found expressed in LB only, intracellularly only, and at both conditions.

Table S2. DEGs of intracellular STM vs. LB.

Table S3. The transcriptome of SPA grown in LB or intracellular. The RNA-seq reads obtained from SPA grown on LB or extracted from HeLa cells infected with SPA were mapped to the SPA 45157 genome. This table shows the normalized (TPM) featurecount counts of reads assigned to the SPA genes. This table also lists the genes that were found expressed in LB only, intracellular only, and under both conditions.

768 **Table S4**. DEGs of intracellular SPA vs. LB.

769 **Table S5**. DEGs between intracellular STM and intracellular SPA.

770 **Table S6**. Bacterial strains and primers utilized in this study.

771 **Table S7**. RNA-Seq metadata and accession numbers of the 12 samples analyzed in this study.

772

773 **MOVIES**

774 **Movie 1. Live-cell imaging of STM and SPA strains reveals intracellular motility of SPA.** To
775 investigate intracellular motility, HeLa cells stably expressing LAMP1-GFP (green) or LifeAct-GFP (green)
776 as indicated were infected with SPA WT, SPA *ssaR*, SPA *fliC*, or STM ATCC 14028s WT, each harboring
777 pFPV-mCherry for constitutive expression of mCherry (red). Individual clips of about 30 seconds are
778 shown successively. Time stamps in upper left corner indicate sec.ms. Scale bars: 10 µm.

779 **Movie 2. Real time imaging of intracellular motility of SPA WT.** HeLa cells stably expressing
780 LifeAct-GFP (green) were infected with SPA WT expression mCherry (red) and imaged at a frame rate of
781 ~40 frames per second. Time stamps in upper left corner indicate sec.ms. Scale bar: 10 µm.

782 **Movie 3. Real time imaging of intracellular motility of SPA WT.** HeLa cells stably expressing
783 LifeAct-GFP (green) were infected with SPA WT expression mCherry (red) and imaged at a frame rate of
784 ~40 frames per second. Time stamps in upper left corner indicate sec.ms. Scale bar: 10 µm.

785 **Movie 4. Live-cell imaging of further intracellular STM and SPA strains.** HeLa cells stably
786 expressing LAMP1-GFP (green) were infected with STM SL1344 WT, or various isolates of SPA as indicated
787 in the lower left corner of movie sections. All strains harbored pFPV-mCherry for constitutive expression
788 of mCherry (red) Time stamps in upper left corner indicate sec.ms. Scale bars: 10 µm.

789

REFERENCES

1. Gal-Mor O. 2019. Persistent Infection and Long-Term Carriage of Typhoidal and Nontyphoidal Salmonellae. Clin Microbiol Rev 32.
2. Kraus MD, Amatya B, Kimula Y. 1999. Histopathology of typhoid enteritis: morphologic and immunophenotypic findings. Mod Pathol 12:949-55.
3. Nguyen QC, Everest P, Tran TK, House D, Murch S, Parry C, Connerton P, Phan VB, To SD, Mastroeni P, White NJ, Tran TH, Vo VH, Dougan G, Farrar JJ, Wain J. 2004. A clinical, microbiological, and pathological study of intestinal perforation associated with typhoid fever. Clin Infect Dis 39:61-7.
4. Sprinz H, Gangarosa EJ, Williams M, Hornick RB, Woodward TE. 1966. Histopathology of the upper small intestines in typhoid fever. Biopsy study of experimental disease in man. Am J Dig Dis 11:615-24.
5. Crump JA, Luby SP, Mintz ED. 2004. The global burden of typhoid fever. Bull World Health Organ 82:346-53.
6. Havelaar AH, Kirk MD, Torgerson PR, Gibb HJ, Hald T, Lake RJ, Praet N, Bellinger DC, de Silva NR, Gargouri N, Speybroeck N, Cawthorne A, Mathers C, Stein C, Angulo FJ, Devleesschauwer B, World Health Organization Foodborne Disease Burden Epidemiology Reference G. 2015. World Health Organization Global Estimates and Regional Comparisons of the Burden of Foodborne Disease in 2010. PLoS Med 12:e1001923.
7. Meltzer E, Schwartz E. 2010. Enteric fever: a travel medicine oriented view. Curr Opin Infect Dis 23:432-7.
8. Ochiai RL, Wang X, von Seidlein L, Yang J, Bhutta ZA, Bhattacharya SK, Agtini M, Deen JL, Wain J, Kim DR, Ali M, Acosta CJ, Jodar L, Clemens JD. 2005. *Salmonella* paratyphi A rates, Asia. Emerg Infect Dis 11:1764-6.
9. Gal-Mor O, Suez J, Elhadad D, Porwollik S, Leshem E, Valinsky L, McClelland M, Schwartz E, Rahav G. 2012. Molecular and cellular characterization of a Salmonella enterica serovar Paratyphi a outbreak strain and the human immune response to infection. Clin Vaccine Immunol 19:146-56.
10. Liu SL, Ezaki T, Miura H, Matsui K, Yabuuchi E. 1988. Intact motility as a *Salmonella typhi* invasion-related factor. Infect Immun 56:1967-73.
11. Abby SS, Rocha EP. 2012. The non-flagellar type III secretion system evolved from the bacterial flagellum and diversified into host-cell adapted systems. PLoS Genet 8:e1002983.
12. Zhou D, Galan J. 2001. *Salmonella* entry into host cells: the work in concert of type III secreted effector proteins. Microbes Infect 3:1293-8.
13. Haraga A, Ohlson MB, Miller SI. 2008. Salmonellae interplay with host cells. Nat Rev Microbiol 6:53-66.
14. Sekirov I, Gill N, Jogova M, Tam N, Robertson M, de Llanos R, Li Y, Finlay BB. 2010. Salmonella SPI-1-mediated neutrophil recruitment during enteric colitis is associated with reduction and alteration in intestinal microbiota. Gut Microbes 1:30-41.
15. Jennings E, Thurston TLM, Holden DW. 2017. Salmonella SPI-2 Type III Secretion System Effectors: Molecular Mechanisms And Physiological Consequences. Cell Host Microbe 22:217-231.
16. Raffatellu M, Chessa D, Wilson RP, Dusold R, Rubino S, Baumler AJ. 2005. The Vi capsular antigen of Salmonella enterica serotype Typhi reduces Toll-like receptor-dependent interleukin-8 expression in the intestinal mucosa. Infect Immun 73:3367-74.
17. Wangdi T, Winter SE, Baumler AJ. 2012. Typhoid fever: "you can't hit what you can't see". Gut Microbes 3:88-92.
18. Winter SE, Winter MG, Thiennimitr P, Gerriets VA, Nuccio SP, Russmann H, Baumler AJ. 2009. The TviA auxiliary protein renders the Salmonella enterica serotype Typhi RcsB regulon responsive to changes in osmolarity. Mol Microbiol 74:175-93.
19. Winter SE, Winter MG, Poon V, Keestra AM, Sterzenbach T, Faber F, Costa LF, Cassou F, Costa EA, Alves GE, Paixao TA, Santos RL, Baumler AJ. 2014. Salmonella enterica Serovar Typhi conceals the invasion-associated type three secretion system from the innate immune system by gene regulation. PLoS Pathog 10:e1004207.
20. Elhadad D, Desai P, Grassl GA, McClelland M, Rahav G, Gal-Mor O. 2016. Differences in Host Cell Invasion and SPI-1 Expression between Salmonella enterica serovar Paratyphi A and the Non-Typhoidal Serovar Typhimurium. Infect Immun doi:10.1128/IAI.01461-15.

21. Elhadad D, Desai P, Rahav G, McClelland M, Gal-Mor O. 2015. Flagellin Is Required for Host Cell Invasion and Normal Salmonella Pathogenicity Island 1 Expression by Salmonella enterica Serovar Paratyphi A. Infect Immun 83:3355-68.
22. Elhadad D, McClelland M, Rahav G, Gal-Mor O. 2015. Feverlike Temperature is a Virulence Regulatory Cue Controlling the Motility and Host Cell Entry of Typhoidal Salmonella. J Infect Dis 212:147-56.
23. McClelland M, Sanderson KE, Spieth J, Clifton SW, Latreille P, Courtney L, Porwollik S, Ali J, Dante M, Du F, Hou S, Layman D, Leonard S, Nguyen C, Scott K, Holmes A, Grewal N, Mulvaney E, Ryan E, Sun H, Florea L, Miller W, Stoneking T, Nhan M, Waterston R, Wilson RK. 2001. Complete genome sequence of *Salmonella enterica* serovar Typhimurium LT2. Nature 413:852-6.
24. Knodler LA, Steele-Mortimer O. 2003. Taking possession: biogenesis of the Salmonella-containing vacuole. Traffic 4:587-99.
25. Kroger C, Colgan A, Srikumar S, Handler K, Sivasankaran SK, Hammarlof DL, Canals R, Grissom JE, Conway T, Hokamp K, Hinton JC. 2013. An infection-relevant transcriptomic compendium for Salmonella enterica Serovar Typhimurium. Cell Host Microbe 14:683-95.
26. Hautefort I, Thompson A, Eriksson-Ygberg S, Parker ML, Lucchini S, Danino V, Bongaerts RJ, Ahmad N, Rhen M, Hinton JC. 2008. During infection of epithelial cells Salmonella enterica serovar Typhimurium undergoes a time-dependent transcriptional adaptation that results in simultaneous expression of three type 3 secretion systems. Cell Microbiol 10:958-84.
27. Liu Y, Yu K, Zhou F, Ding T, Yang Y, Hu M, Liu X. 2017. Quantitative Proteomics Charts the Landscape of Salmonella Carbon Metabolism within Host Epithelial Cells. J Proteome Res 16:788-797.
28. Deiwick J, Nikolaus T, Erdogan S, Hensel M. 1999. Environmental regulation of Salmonella pathogenicity island 2 gene expression. Mol Microbiol 31:1759-73.
29. Prost LR, Miller SI. 2008. The Salmonellae PhoQ sensor: mechanisms of detection of phagosome signals. Cell Microbiol 10:576-82.
30. Hensel M, Shea JE, Waterman SR, Mundy R, Nikolaus T, Banks G, Vazquez-Torres A, Gleeson C, Fang FC, Holden DW. 1998. Genes encoding putative effector proteins of the type III secretion system of Salmonella pathogenicity island 2 are required for bacterial virulence and proliferation in macrophages. Mol Microbiol 30:163-74.
31. Eriksson S, Lucchini S, Thompson A, Rhen M, Hinton JC. 2003. Unravelling the biology of macrophage infection by gene expression profiling of intracellular Salmonella enterica. Mol Microbiol 47:103-18.
32. Srikumar S, Kroger C, Hebrard M, Colgan A, Owen SV, Sivasankaran SK, Cameron AD, Hokamp K, Hinton JC. 2015. RNA-seq Brings New Insights to the Intra-Macrophage Transcriptome of Salmonella Typhimurium. PLoS Pathog 11:e1005262.
33. Ratledge C. 2007. Iron metabolism and infection. Food Nutr Bull 28:S515-23.
34. Brown SA, Palmer KL, Whiteley M. 2008. Revisiting the host as a growth medium. Nat Rev Microbiol 6:657-66.
35. Eisenreich W, Dandekar T, Heesemann J, Goebel W. 2010. Carbon metabolism of intracellular bacterial pathogens and possible links to virulence. Nat Rev Microbiol 8:401-12.
36. Brzoska P, Boos W. 1988. Characteristics of a ugp-encoded and phoB-dependent glycerophosphoryl diester phosphodiesterase which is physically dependent on the ugp transport system of Escherichia coli. J Bacteriol 170:4125-35.
37. Conlin CA, Tan SL, Hu H, Segar T. 2001. The apeE gene of Salmonella enterica serovar Typhimurium is induced by phosphate limitation and regulated by phoBR. J Bacteriol 183:1784-6.
38. Jiang W, Metcalf WW, Lee KS, Wanner BL. 1995. Molecular cloning, mapping, and regulation of Pho regulon genes for phosphonate breakdown by the phosphonatase pathway of Salmonella typhimurium LT2. J Bacteriol 177:6411-21.
39. Bowden SD, Rowley G, Hinton JC, Thompson A. 2009. Glucose and glycolysis are required for the successful infection of macrophages and mice by Salmonella enterica serovar typhimurium. Infect Immun 77:3117-26.

40. Bowden SD, Hopper-Chidlaw AC, Rice CJ, Ramachandran VK, Kelly DJ, Thompson A. 2014. Nutritional and metabolic requirements for the infection of HeLa cells by Salmonella enterica serovar Typhimurium. PLoS One 9:e96266.
41. Lundberg BE, Wolf RE, Jr., Dinauer MC, Xu Y, Fang FC. 1999. Glucose 6-phosphate dehydrogenase is required for Salmonella typhimurium virulence and resistance to reactive oxygen and nitrogen intermediates. Infect Immun 67:436-8.
42. Romero M, Laorden ML, Hernandez J, Serrano JS. 1991. Evidence for involvement of catecholamines in the effect of morphine on ventricular automaticity in the rat. J Auton Pharmacol 11:93-9.
43. Tchawa Yimga M, Leatham MP, Allen JH, Laux DC, Conway T, Cohen PS. 2006. Role of gluconeogenesis and the tricarboxylic acid cycle in the virulence of Salmonella enterica serovar Typhimurium in BALB/c mice. Infect Immun 74:1130-40.
44. Gotz A, Goebel W. 2010. Glucose and glucose 6-phosphate as carbon sources in extra- and intracellular growth of enteroinvasive Escherichia coli and Salmonella enterica. Microbiology (Reading) 156:1176-1187.
45. Holt KE, Thomson NR, Wain J, Langridge GC, Hasan R, Bhutta ZA, Quail MA, Norbertczak H, Walker D, Simmonds M, White B, Bason N, Mungall K, Dougan G, Parkhill J. 2009. Pseudogene accumulation in the evolutionary histories of Salmonella enterica serovars Paratyphi A and Typhi. BMC Genomics 10:36.
46. Kaval KG, Garsin DA. 2018. Ethanolamine Utilization in Bacteria. mBio 9.
47. Kofoid E, Rappleye C, Stojiljkovic I, Roth J. 1999. The 17-gene ethanolamine (eut) operon of Salmonella typhimurium encodes five homologues of carboxysome shell proteins. J Bacteriol 181:5317-29.
48. Horstmann JA, Zschieschang E, Truschel T, de Diego J, Lunelli M, Rohde M, May T, Strowig T, Stradal T, Kolbe M, Erhardt M. 2017. Flagellin phase-dependent swimming on epithelial cell surfaces contributes to productive Salmonella gut colonisation. Cell Microbiol 19.
49. Misselwitz B, Barrett N, Kreibich S, Vonaesch P, Andritschke D, Rout S, Weidner K, Sormaz M, Songhet P, Horvath P, Chabria M, Vogel V, Spori DM, Jenny P, Hardt WD. 2012. Near surface swimming of Salmonella Typhimurium explains target-site selection and cooperative invasion. PLoS Pathog 8:e1002810.
50. Chilcott GS, Hughes KT. 2000. Coupling of flagellar gene expression to flagellar assembly in Salmonella enterica serovar typhimurium and Escherichia coli. Microbiol Mol Biol Rev 64:694-708.
51. Reuter T, Scharte F, Franzkoch R, Liss V, Hensel M. 2021. Single cell analyses reveal distinct adaptation of typhoidal and non-typhoidal Salmonella enterica serovars to intracellular lifestyle. PLoS Pathog 17:e1009319.
52. Welch MD, Way M. 2013. Arp2/3-mediated actin-based motility: a tail of pathogen abuse. Cell Host Microbe 14:242-55.
53. Pizarro-Cerda J, Cossart P. 2018. Listeria monocytogenes: cell biology of invasion and intracellular growth. Microbiol Spectr 6.
54. Boyd EF, Wang FS, Beltran P, Plock SA, Nelson K, Selander RK. 1993. Salmonella reference collection B (SARB): strains of 37 serovars of subspecies I. J Gen Microbiol 139 Pt 6:1125-32.
55. Ibarra JA, Knodler LA, Sturdevant DE, Virtaneva K, Carmody AB, Fischer ER, Porcella SF, Steele-Mortimer O. 2010. Induction of *Salmonella* pathogenicity island 1 under different growth conditions can affect Salmonella-host cell interactions in vitro. Microbiology 156:1120-33.
56. Gal-Mor O, Boyle EC, Grassl GA. 2014. Same species, different diseases: how and why typhoidal and non-typhoidal Salmonella enterica serovars differ. Front Microbiol 5:391.
57. Hoiseth SK, Stocker BA. 1981. Aromatic-dependent *Salmonella typhimurium* are non-virulent and effective as live vaccines. Nature 291:238-9.
58. Fields PI, Swanson RV, Haidaris CG, Heffron F. 1986. Mutants of *Salmonella typhimurium* that cannot survive within the macrophage are avirulent. Proc Natl Acad Sci U S A 83:5189-93.
59. McFarland WC, Stocker BA. 1987. Effect of different purine auxotrophic mutations on mouse-virulence of a Vi-positive strain of Salmonella dublin and of two strains of Salmonella typhimurium. Microb Pathog 3:129-41.
60. O'Callaghan D, Maskell D, Liew FY, Easmon CS, Dougan G. 1988. Characterization of aromatic- and purine-dependent Salmonella typhimurium: attention, persistence, and ability to induce protective immunity in BALB/c mice. Infect Immun 56:419-23.

61. Liu Y, Zhang Q, Hu M, Yu K, Fu J, Zhou F, Liu X. 2015. Proteomic Analyses of Intracellular Salmonella enterica Serovar Typhimurium Reveal Extensive Bacterial Adaptations to Infected Host Epithelial Cells. Infect Immun 83:2897-906.
62. Osman D, Cavet JS. 2011. Metal sensing in Salmonella: implications for pathogenesis. Adv Microb Physiol 58:175-232.
63. Ammendola S, Pasquali P, Pistoia C, Petrucci P, Petrarca P, Rotilio G, Battistoni A. 2007. High-affinity Zn2+ uptake system ZnuABC is required for bacterial zinc homeostasis in intracellular environments and contributes to the virulence of Salmonella enterica. Infect Immun 75:5867-76.
64. Schaible UE, Kaufmann SH. 2004. Iron and microbial infection. Nat Rev Microbiol 2:946-53.
65. Finlay BB, Chatfield S, Leung KY, Dougan G, Falkow S. 1991. Characterization of a Salmonella choleraesuis mutant that cannot multiply within epithelial cells. Can J Microbiol 37:568-72.
66. Denkel LA, Rhen M, Bange FC. 2013. Biotin sulfoxide reductase contributes to oxidative stress tolerance and virulence in Salmonella enterica serovar Typhimurium. Microbiology (Reading) 159:1447-1458.
67. Bakovic M, Fullerton MD, Michel V. 2007. Metabolic and molecular aspects of ethanolamine phospholipid biosynthesis: the role of CTP:phosphoethanolamine cytidylyltransferase (Pcyt2). Biochem Cell Biol 85:283-300.
68. Garsin DA. 2010. Ethanolamine utilization in bacterial pathogens: roles and regulation. Nat Rev Microbiol 8:290-5.
69. Joseph B, Przybilla K, Stuhler C, Schauer K, Slaghuis J, Fuchs TM, Goebel W. 2006. Identification of Listeria monocytogenes genes contributing to intracellular replication by expression profiling and mutant screening. J Bacteriol 188:556-68.
70. Thiennimitr P, Winter SE, Winter MG, Xavier MN, Tolstikov V, Huseby DL, Sterzenbach T, Tsolis RM, Roth JR, Baumler AJ. 2011. Intestinal inflammation allows Salmonella to use ethanolamine to compete with the microbiota. Proc Natl Acad Sci U S A 108:17480-5.
71. Singh B, Arya G, Kundu N, Sangwan A, Nongthombam S, Chaba R. 2019. Molecular and Functional Insights into the Regulation of d-Galactonate Metabolism by the Transcriptional Regulator DgoR in Escherichia coli. J Bacteriol 201.
72. Arunima A, Yelamanchi SD, Padhi C, Jaiswal S, Ryan D, Gupta B, Sathe G, Advani J, Gowda H, Prasad TSK, Suar M. 2017. "Omics" of Food-Borne Gastroenteritis: Global Proteomic and Mutagenic Analysis of Salmonella enterica Serovar Enteritidis. OMICS 21:571-583.
73. Utley M, Franklin DP, Krogfelt KA, Laux DC, Cohen PS. 1998. A Salmonella typhimurium mutant unable to utilize fatty acids and citrate is avirulent and immunogenic in mice. FEMS Microbiol Lett 163:129-34.
74. Nunez-Hernandez C, Tierrez A, Ortega AD, Pucciarelli MG, Godoy M, Eisman B, Casadesus J, Garcia-del Portillo F. 2013. Genome expression analysis of nonproliferating intracellular Salmonella enterica serovar Typhimurium unravels an acid pH-dependent PhoP-PhoQ response essential for dormancy. Infect Immun 81:154-65.
75. Schmitt CK, Ikeda JS, Darnell SC, Watson PR, Bispham J, Wallis TS, Weinstein DL, Metcalf ES, O'Brien AD. 2001. Absence of all components of the flagellar export and synthesis machinery differentially alters virulence of *Salmonella enterica* serovar Typhimurium in models of typhoid fever, survival in macrophages, tissue culture invasiveness, and calf enterocolitis. Infect Immun 69:5619-25.
76. Stecher B, Hapfelmeier S, Muller C, Kremer M, Stallmach T, Hardt WD. 2004. Flagella and chemotaxis are required for efficient induction of Salmonella enterica serovar Typhimurium colitis in streptomycin-pretreated mice. Infect Immun 72:4138-50.
77. Lin D, Rao CV, Slauch JM. 2008. The Salmonella SPI1 type three secretion system responds to periplasmic disulfide bond status via the flagellar apparatus and the RcsCDB system. J Bacteriol 190:87-97.
78. Boddicker JD, Jones BD. 2004. Lon protease activity causes down-regulation of Salmonella pathogenicity island 1 invasion gene expression after infection of epithelial cells. Infect Immun 72:2002-13.
79. Nunez-Hernandez C, Alonso A, Pucciarelli MG, Casadesus J, Garcia-del Portillo F. 2014. Dormant intracellular Salmonella enterica serovar Typhimurium discriminates among Salmonella pathogenicity island 2 effectors to persist inside fibroblasts. Infect Immun 82:221-32.

80. Fattinger SA, Sellin ME, Hardt WD. 2021. Epithelial inflammasomes in the defense against Salmonella gut infection. Curr Opin Microbiol 59:86-94.
81. Kuehl CJ, Dragoi AM, Talman A, Agaisse H. 2015. Bacterial spread from cell to cell: beyond actin-based motility. Trends Microbiol 23:558-66.
82. Knodler LA, Vallance BA, Celli J, Winfree S, Hansen B, Montero M, Steele-Mortimer O. 2010. Dissemination of invasive Salmonella via bacterial-induced extrusion of mucosal epithelia. Proc Natl Acad Sci U S A 107:17733-8.
83. Dutta D, Clevers H. 2017. Organoid culture systems to study host-pathogen interactions. Curr Opin Immunol 48:15-22.
84. Sepe LP, Hartl K, Iftekhar A, Berger H, Kumar N, Goosmann C, Chopra S, Schmidt SC, Gurumurthy RK, Meyer TF, Boccellato F. 2020. Genotoxic Effect of Salmonella Paratyphi A Infection on Human Primary Gallbladder Cells. mBio 11.
85. Jarvik T, Smillie C, Groisman EA, Ochman H. 2010. Short-term signatures of evolutionary change in the Salmonella enterica serovar typhimurium 14028 genome. J Bacteriol 192:560-7.
86. Lorkowski M, Felipe-Lopez A, Danzer CA, Hansmeier N, Hensel M. 2014. Salmonella enterica invasion of polarized epithelial cells is a highly cooperative effort. Infect Immun 82:2657-67.
87. Westermann AJ, Gorski SA, Vogel J. 2012. Dual RNA-seq of pathogen and host. Nat Rev Microbiol 10:618-30.
88. Kopylova E, Noe L, Touzet H. 2012. SortMeRNA: fast and accurate filtering of ribosomal RNAs in metatranscriptomic data. Bioinformatics 28:3211-7.
89. Sallet E, Gouzy J, Schiex T. 2014. EuGene-PP: a next-generation automated annotation pipeline for prokaryotic genomes. Bioinformatics 30:2659-61.
90. Galperin MY, Makarova KS, Wolf YI, Koonin EV. 2015. Expanded microbial genome coverage and improved protein family annotation in the COG database. Nucleic Acids Res 43:D261-9.
91. Roberts RJ, Vincze T, Posfai J, Macelis D. 2010. REBASE--a database for DNA restriction and modification: enzymes, genes and genomes. Nucleic Acids Res 38:D234-6.
92. Bertelli C, Laird MR, Williams KP, Simon Fraser University Research Computing G, Lau BY, Hoad G, Winsor GL, Brinkman FSL. 2017. IslandViewer 4: expanded prediction of genomic islands for larger-scale datasets. Nucleic Acids Res 45:W30-W35.
93. Zhou Y, Liang Y, Lynch KH, Dennis JJ, Wishart DS. 2011. PHAST: a fast phage search tool. Nucleic Acids Res 39:W347-52.
94. Cros MJ, de Monte A, Mariette J, Bardou P, Grenier-Boley B, Gautheret D, Touzet H, Gaspin C. 2011. RNAspace.org: An integrated environment for the prediction, annotation, and analysis of ncRNA. RNA 17:1947-56.
95. Lagesen K, Hallin P, Rodland EA, Staerfeldt HH, Rognes T, Ussery DW. 2007. RNAmmer: consistent and rapid annotation of ribosomal RNA genes. Nucleic Acids Res 35:3100-8.
96. Chan PP, Lowe TM. 2019. tRNAscan-SE: Searching for tRNA Genes in Genomic Sequences. Methods Mol Biol 1962:1-14.
97. Gardner PP, Daub J, Tate JG, Nawrocki EP, Kolbe DL, Lindgreen S, Wilkinson AC, Finn RD, Griffiths-Jones S, Eddy SR, Bateman A. 2009. Rfam: updates to the RNA families database. Nucleic Acids Res 37:D136-40.
98. Quinlan AR, Hall IM. 2010. BEDTools: a flexible suite of utilities for comparing genomic features. Bioinformatics 26:841-2.
99. Dobin A, Davis CA, Schlesinger F, Drenkow J, Zaleski C, Jha S, Batut P, Chaisson M, Gingeras TR. 2013. STAR: ultrafast universal RNA-seq aligner. Bioinformatics 29:15-21.
100. Liao Y, Smyth GK, Shi W. 2014. featureCounts: an efficient general purpose program for assigning sequence reads to genomic features. Bioinformatics 30:923-30.
101. Page AJ, Cummins CA, Hunt M, Wong VK, Reuter S, Holden MT, Fookes M, Falush D, Keane JA, Parkhill J. 2015. Roary: rapid large-scale prokaryote pan genome analysis. Bioinformatics 31:3691-3.
102. Boddu D, George R, Nair S, Bindra M, L GM. 2014. Hydroa Vacciniforme-Like Lymphoma: A Case Report From India. J Pediatr Hematol Oncol doi:10.1097/MPH.0000000000000221.

041 103. Gu Z, Eils R, Schlesner M. 2016. Complex heatmaps reveal patterns and correlations in multidimensional
042 genomic data. Bioinformatics 32:2847-9.
043 104. Aviv G, Gal-Mor O. 2018. Western Blotting Against Tagged Virulence Determinants to Study Bacterial
044 Pathogenicity. Methods Mol Biol 1734:47-54.

045

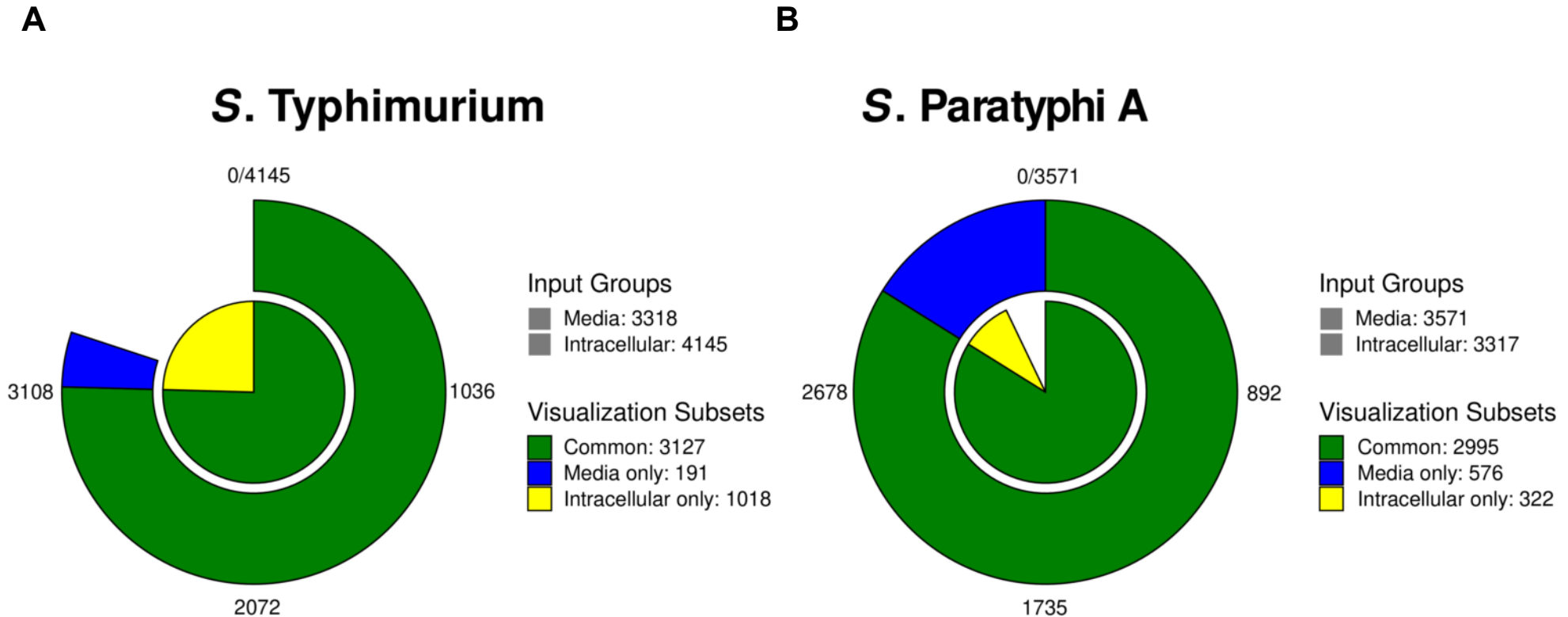
A
S. Typhimurium
0/4145
3108
1036
2072
Input Groups
Media: 3318
Intracellular: 4145
Visualization Subsets
Common: 3127
Media only: 191
Intracellular only: 1018
B
S. Paratyphi A
0/3571
2678
892
1735
Input Groups
Media: 3571
Intracellular: 3317
Visualization Subsets
Common: 2995
Media only: 576
Intracellular only: 322

Fig. 1

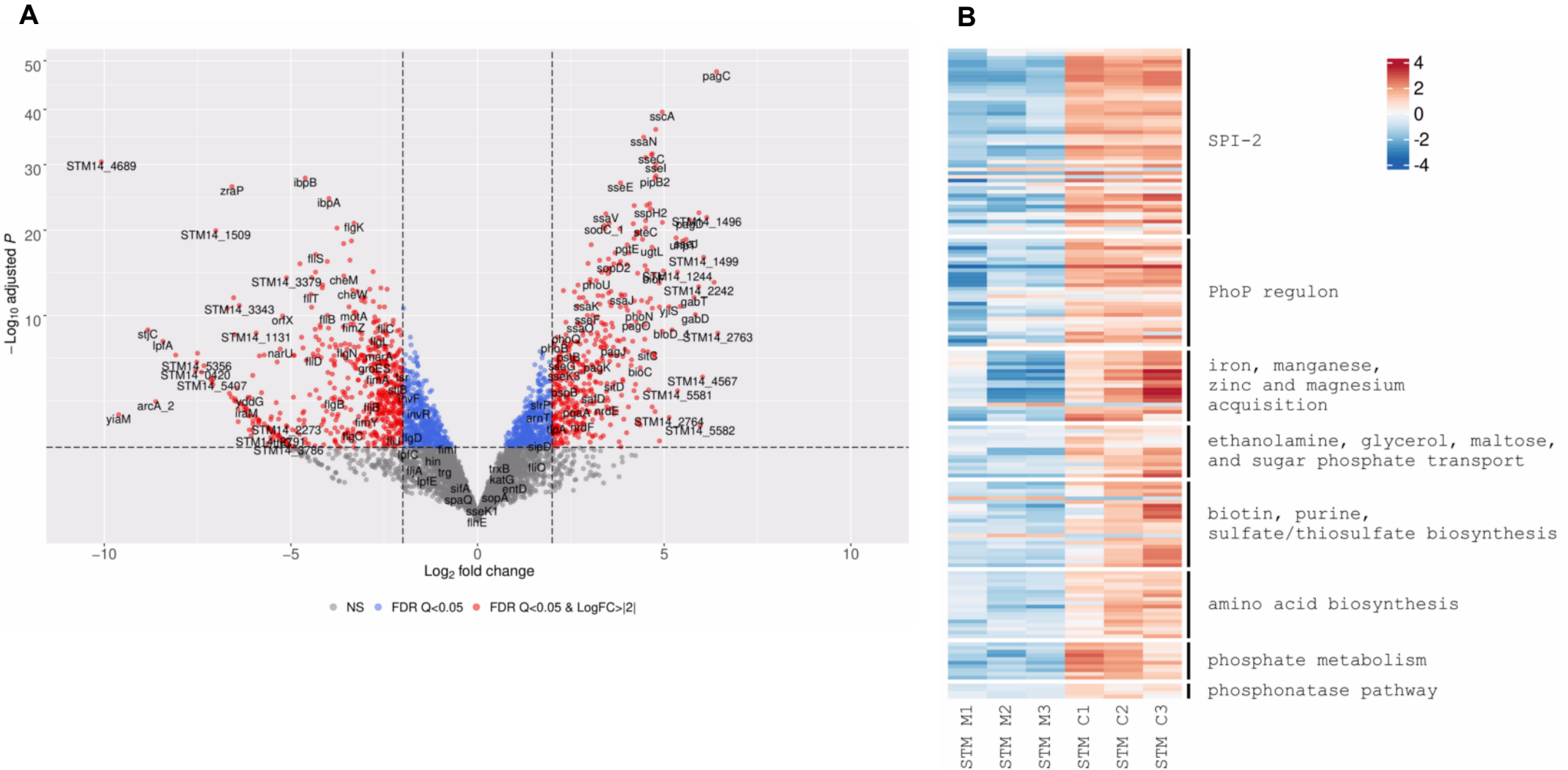
A
B
−Log10 adjusted P
Log2 fold change
NS
FDR Q<0.05
FDR Q<0.05 & LogFC>|2|
SPI-2
PhoP regulon
iron, manganese, zinc and magnesium acquisition
ethanolamine, glycerol, maltose, and sugar phosphate transport
biotin, purine, sulfate/thiosulfate biosynthesis
amino acid biosynthesis
phosphate metabolism
phosphonatase pathway
STM M1
STM M2
STM M3
STM C1
STM C2
STM C3

Fig. 2

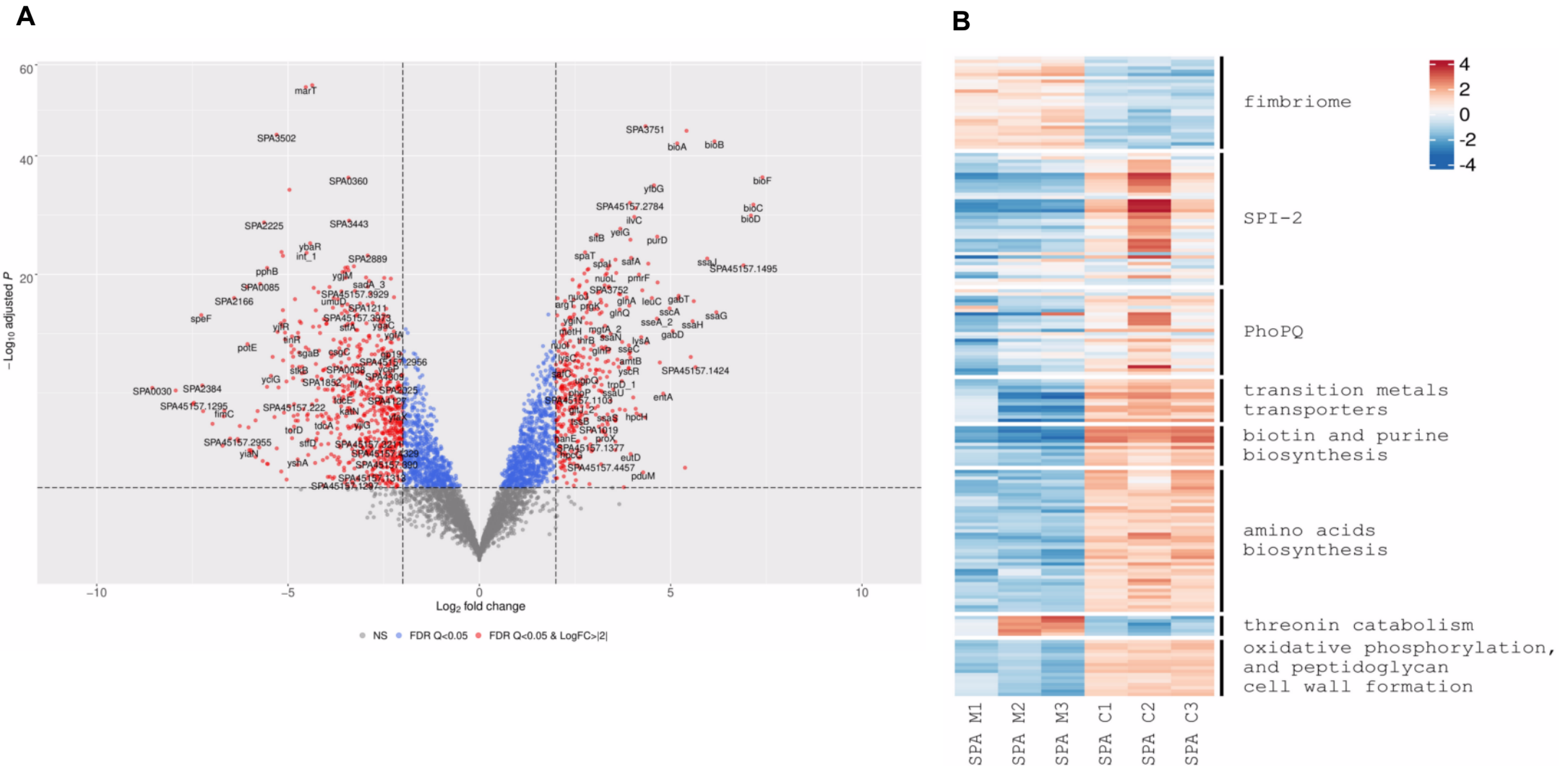
A
B
−Log10 adjusted P
Log2 fold change
NS
FDR Q<0.05
FDR Q<0.05 & LogFC>|2|
fimbriome
SPI-2
PhoPQ
transition metals transporters
biotin and purine biosynthesis
amino acids biosynthesis
threonin catabolism
oxidative phosphorylation, and peptidoglycan cell wall formation
SPA M1
SPA M2
SPA M3
SPA C1
SPA C2
SPA C3

Fig. 3

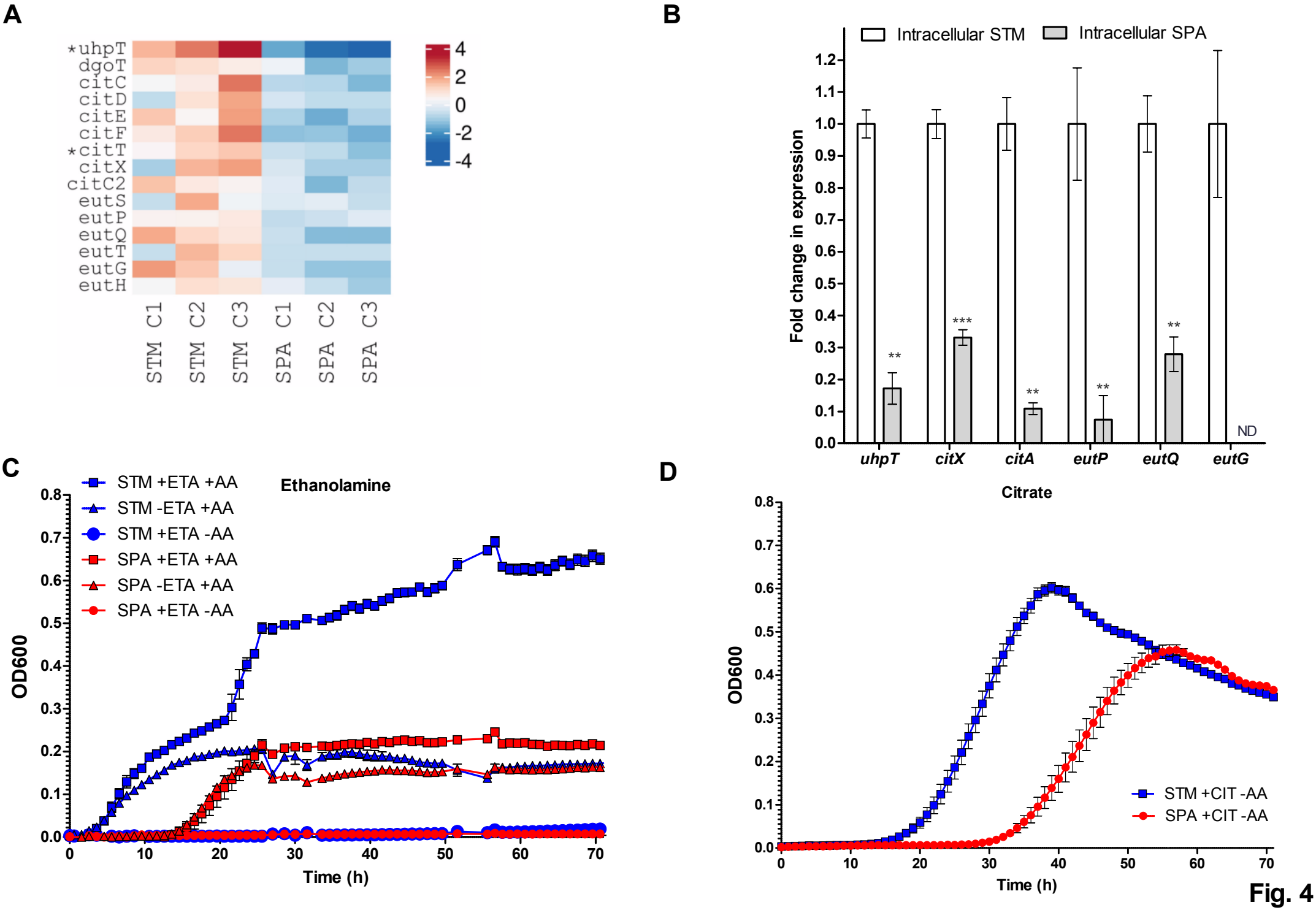
A
*uhpT
dgoT
citC
citD
citE
citF
*citT
citX
citC2
eutS
eutP
eutQ
eutT
eutG
eutH
STM C1
STM C2
STM C3
SPA C1
SPA C2
SPA C3
4
2
0
-2
-4
B
Intracellular STM
Intracellular SPA
Fold change in expression
uhpT
citX
citA
eutP
eutQ
eutG
ND
C
Ethanolamine
STM +ETA +AA
STM -ETA +AA
STM +ETA -AA
SPA +ETA +AA
SPA -ETA +AA
SPA +ETA -AA
OD600
Time (h)
D
Citrate
STM +CIT -AA
SPA +CIT -AA
OD600
Time (h)

Fig. 4

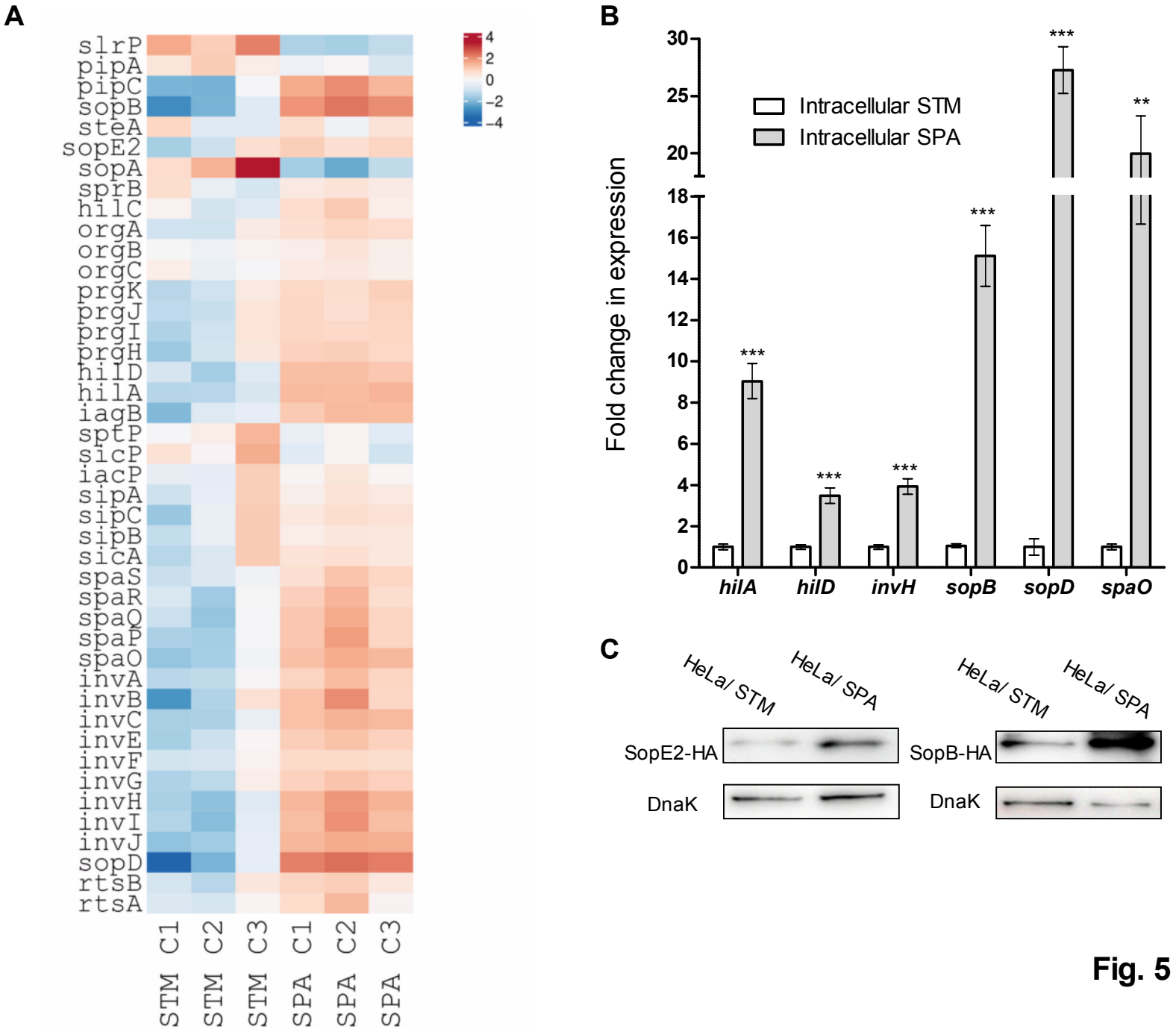
A
slrP
pipA
pipC
sopB
steA
sopE2
sopA
sprB
hilC
orgA
orgB
orgC
prgK
prgJ
prgI
prgH
hilD
hilA
iagB
sptP
sicP
iacP
sipA
sipC
sipB
sicA
spaS
spaR
spaQ
spaP
spaO
invA
invB
invC
invE
invF
invG
invH
invI
invJ
sopD
rtsB
rtsA
4
2
0
−2
−4
STM C1
STM C2
STM C3
SPA C1
SPA C2
SPA C3
B
Fold change in expression
Intracellular STM
Intracellular SPA
30
25
20
18
16
14
12
10
8
6
4
2
0
***
***
***
***
***
**
hilA
hilD
invH
sopB
sopD
spaO
C
HeLa/ STM
HeLa/ SPA
HeLa/ STM
HeLa/ SPA
SopE2-HA
SopB-HA
DnaK
DnaK

Fig. 5

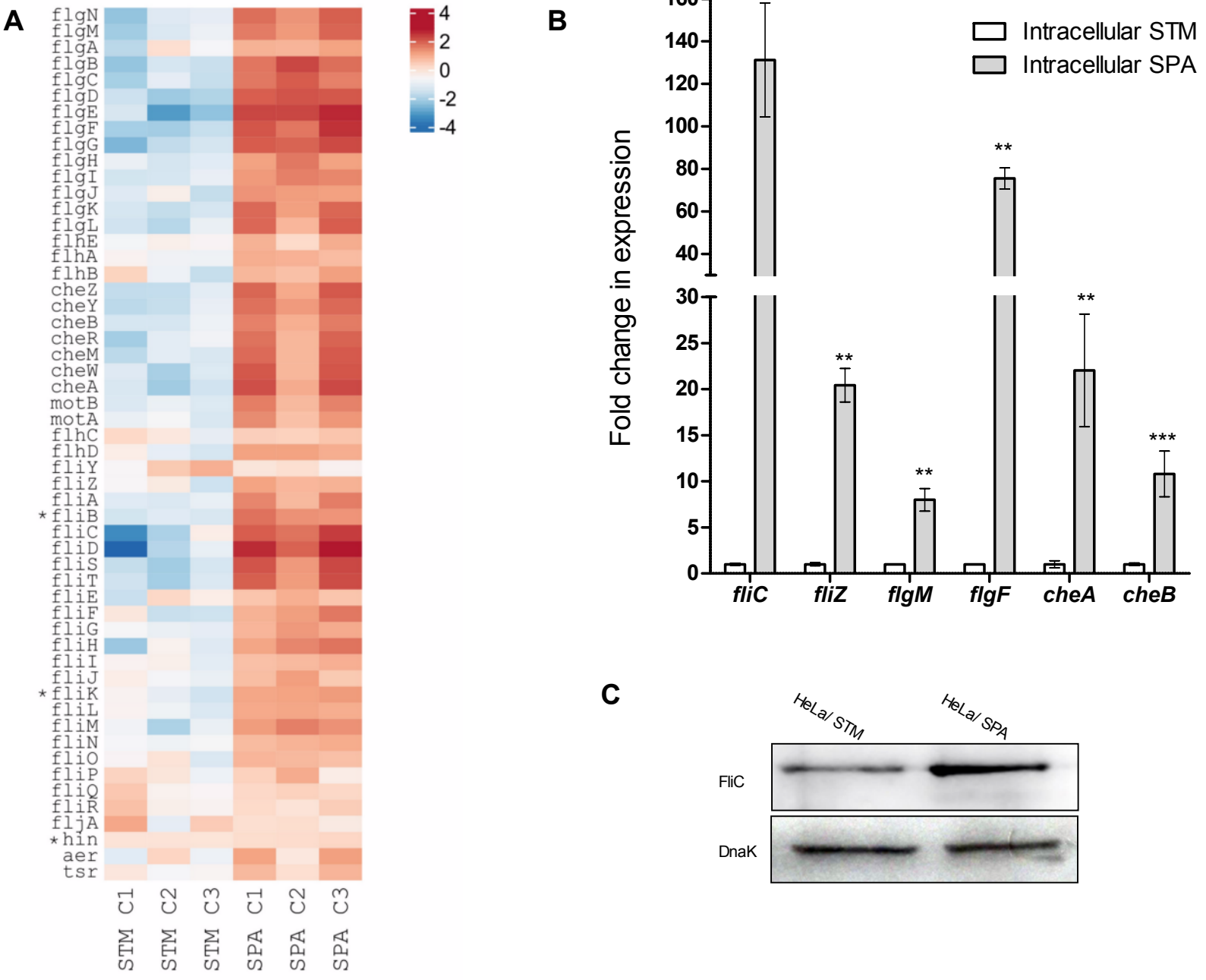
A
flgN
flgM
flgA
flgB
flgC
flgD
flgE
flgF
flgG
flgH
flgI
flgJ
flgK
flgL
flhE
flhA
flhB
cheZ
cheY
cheB
cheR
cheM
cheW
cheA
motB
motA
flhC
flhD
fliY
fliZ
fliA
*fliB
fliC
fliD
fliS
fliT
fliE
fliF
fliG
fliH
fliI
fliJ
*fliK
fliL
fliM
fliN
fliO
fliP
fliQ
fliR
fljA
*hin
aer
tsr
4
2
0
-2
-4
STM C1
STM C2
STM C3
SPA C1
SPA C2
SPA C3
B
Intracellular STM
Intracellular SPA
Fold change in expression
160
140
120
100
80
60
40
30
25
20
15
10
5
0
**
**
**
**
**
***
fliC
fliZ
flgM
flgF
cheA
cheB
C
HeLa/ STM
HeLa/ SPA
FliC
DnaK

Fig. 6

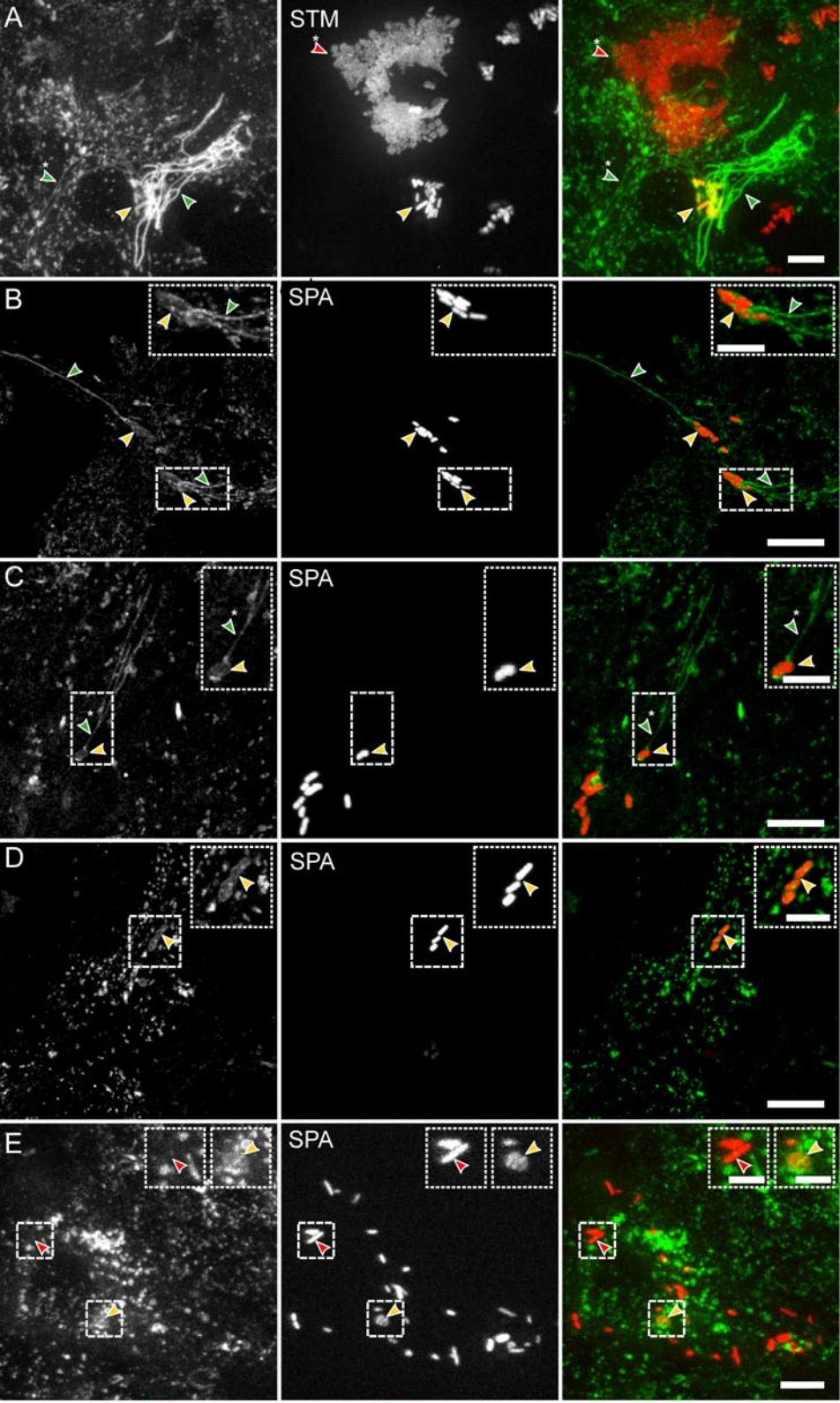
A
STM
B
SPA
C
SPA
D
SPA
E
SPA
LAMP1
Salmonella
merge

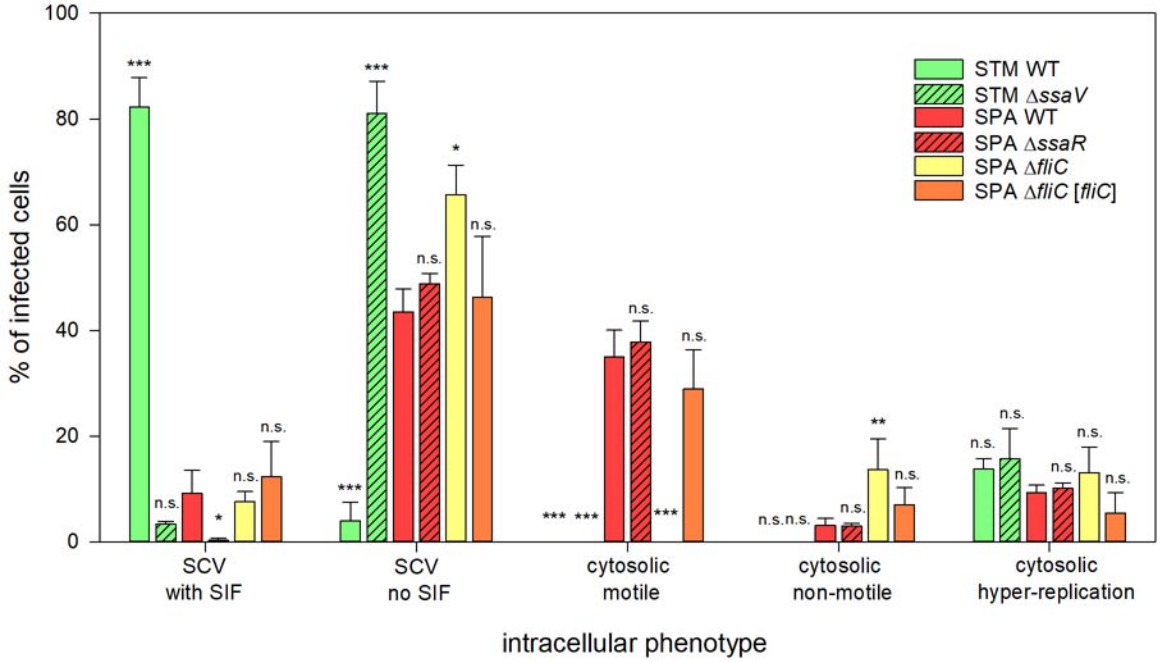
% of infected cells
100
80
60
40
20
0
STM WT
STM ΔssaV
SPA WT
SPA ΔssaR
SPA ΔfliC
SPA ΔfliC [fliC]
***
n.s.
*
n.s.
n.s.
***
***
n.s.
n.s.
*
n.s.
***
***
***
n.s.
n.s.
n.s.
n.s.
n.s.
**
n.s.
n.s.
n.s.
n.s.
n.s.
n.s.
SCV with SIF
SCV no SIF
cytosolic motile
cytosolic non-motile
cytosolic hyper-replication
intracellular phenotype

A

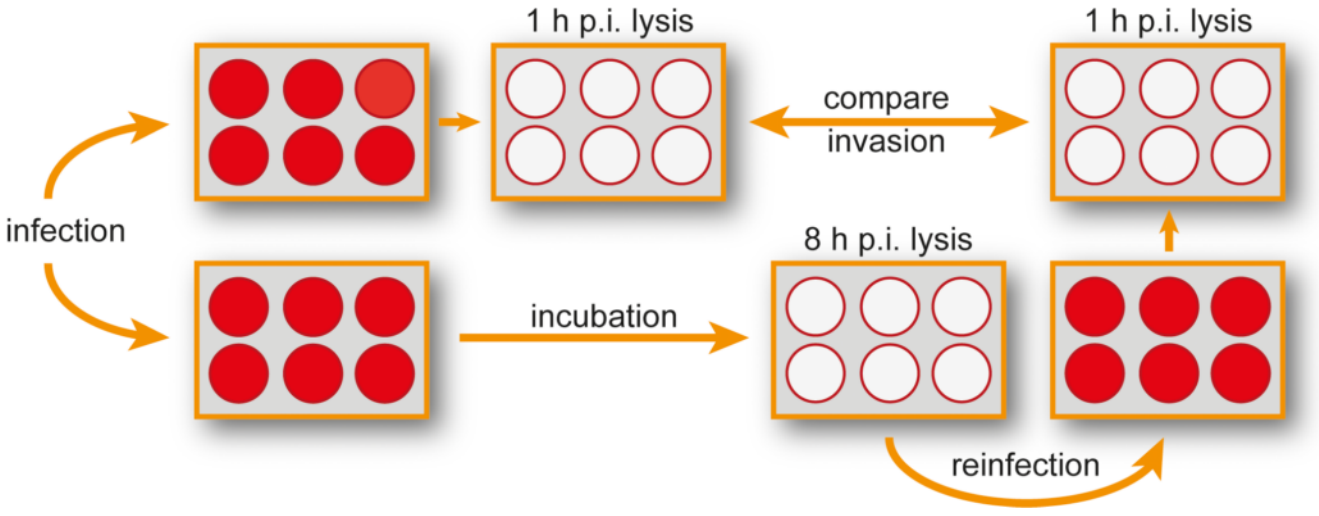
1 h p.i. lysis
1 h p.i. lysis
compare
invasion
infection
8 h p.i. lysis
incubation
reinfection

B

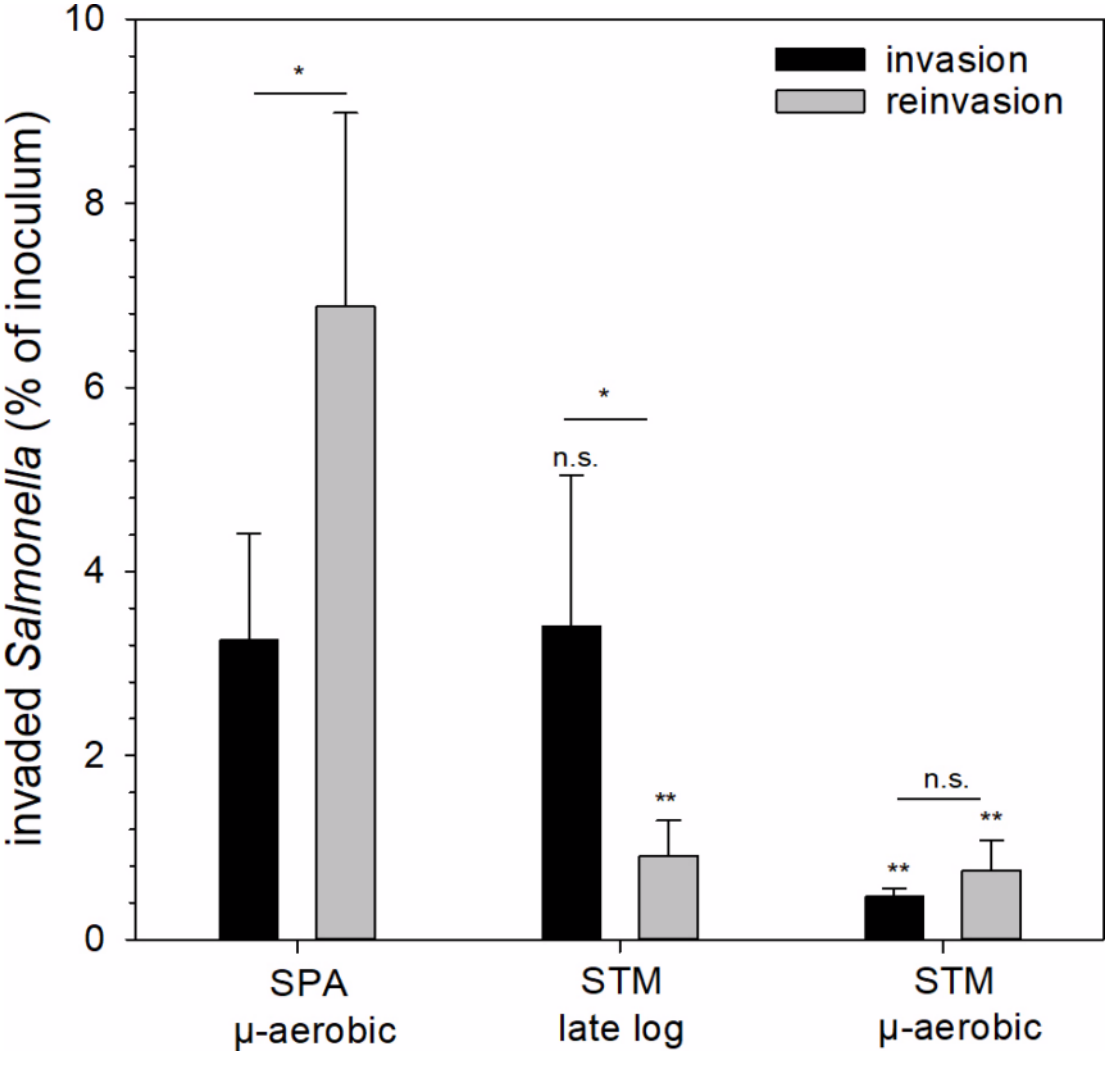
invaded Salmonella (% of inoculum)
10
8
6
4
2
0
invasion
reinvasion
*
*
n.s.
**
n.s.
**
**
SPA
μ-aerobic
STM
late log
STM
μ-aerobic

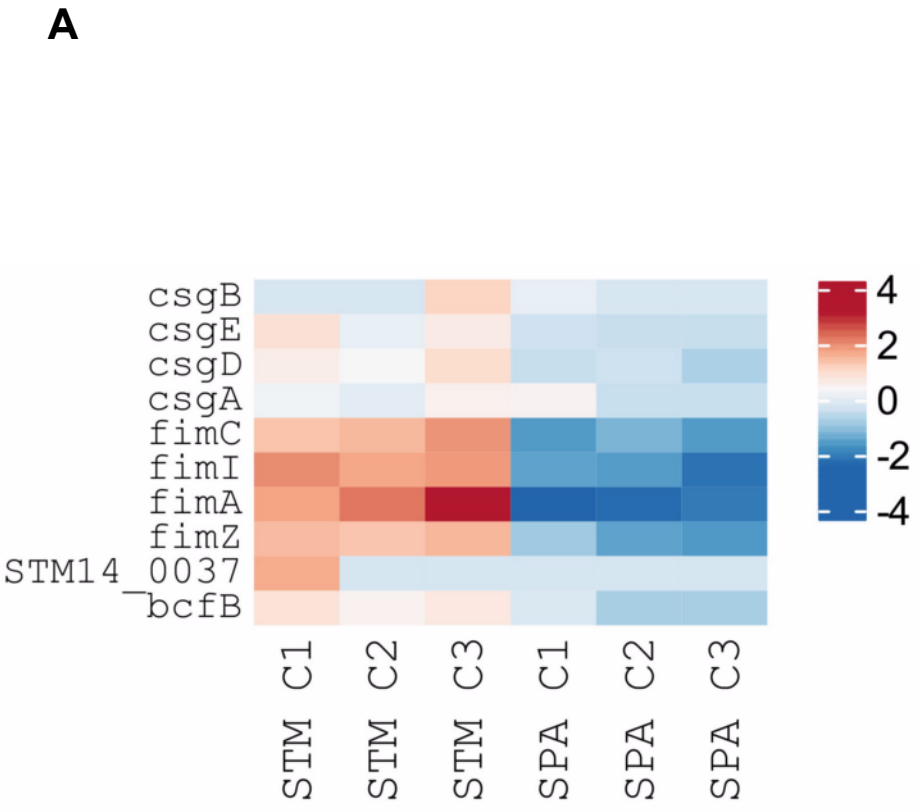
A
csgB
csgE
csgD
csgA
fimC
fimI
fimA
fimZ
STM14_0037
bcfB
STM C1
STM C2
STM C3
SPA C1
SPA C2
SPA C3
4
2
0
-2
-4

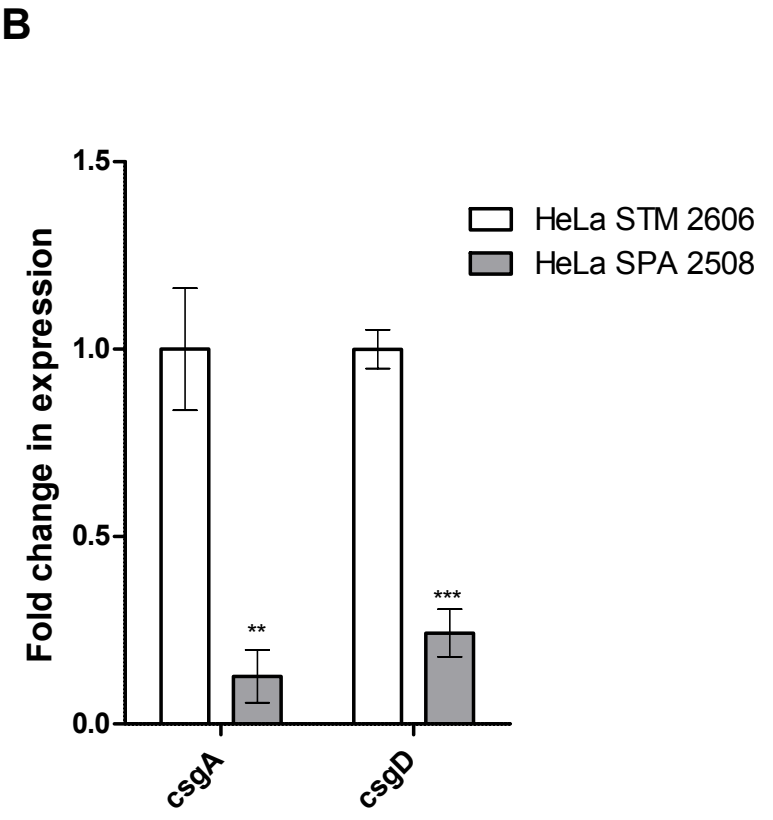
B
Fold change in expression
1.5
1.0
0.5
0.0
HeLa STM 2606
HeLa SPA 2508
**
***
csgA
csgD

Fig. S1

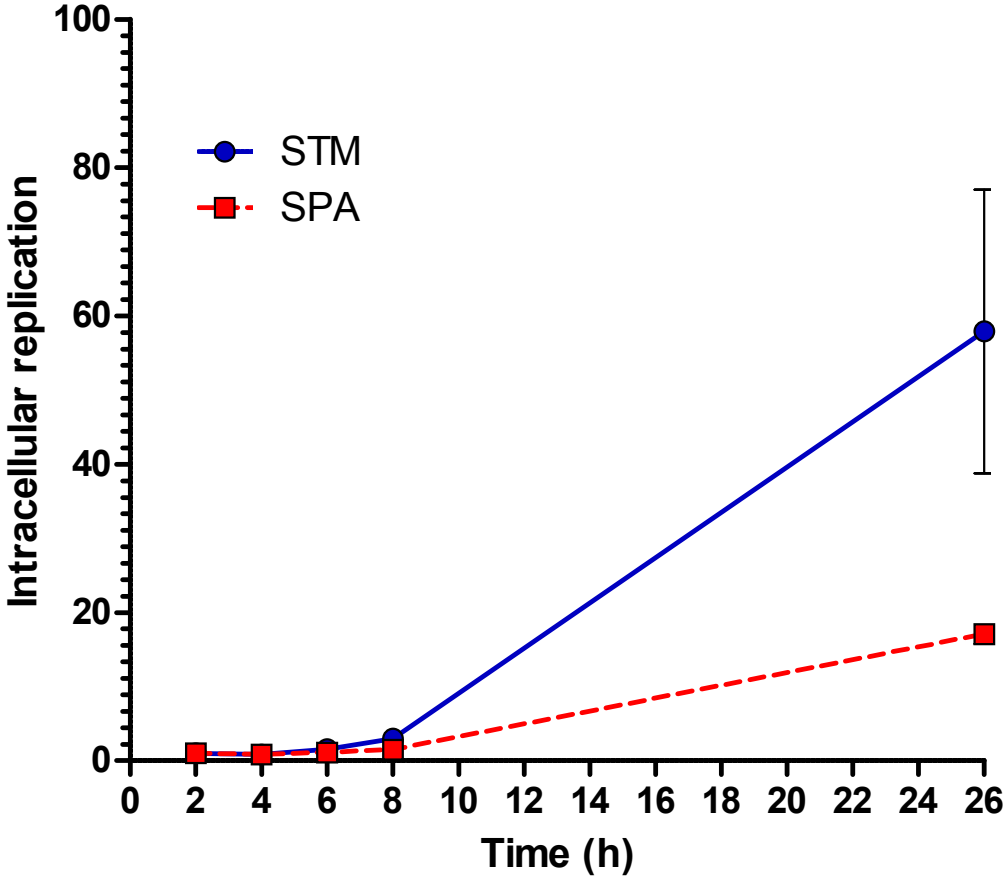
100
80
60
40
20
0
Intracellular replication
STM
SPA
0
2
4
6
8
10
12
14
16
18
20
22
24
26
Time (h)

Fig. S2

SPA WT

SPA *fliC*

SPA *fliC* [*fliC*]

STM WT

STM *fliC fljB*

LAMP1 | *Salmonella* | flagella | merge

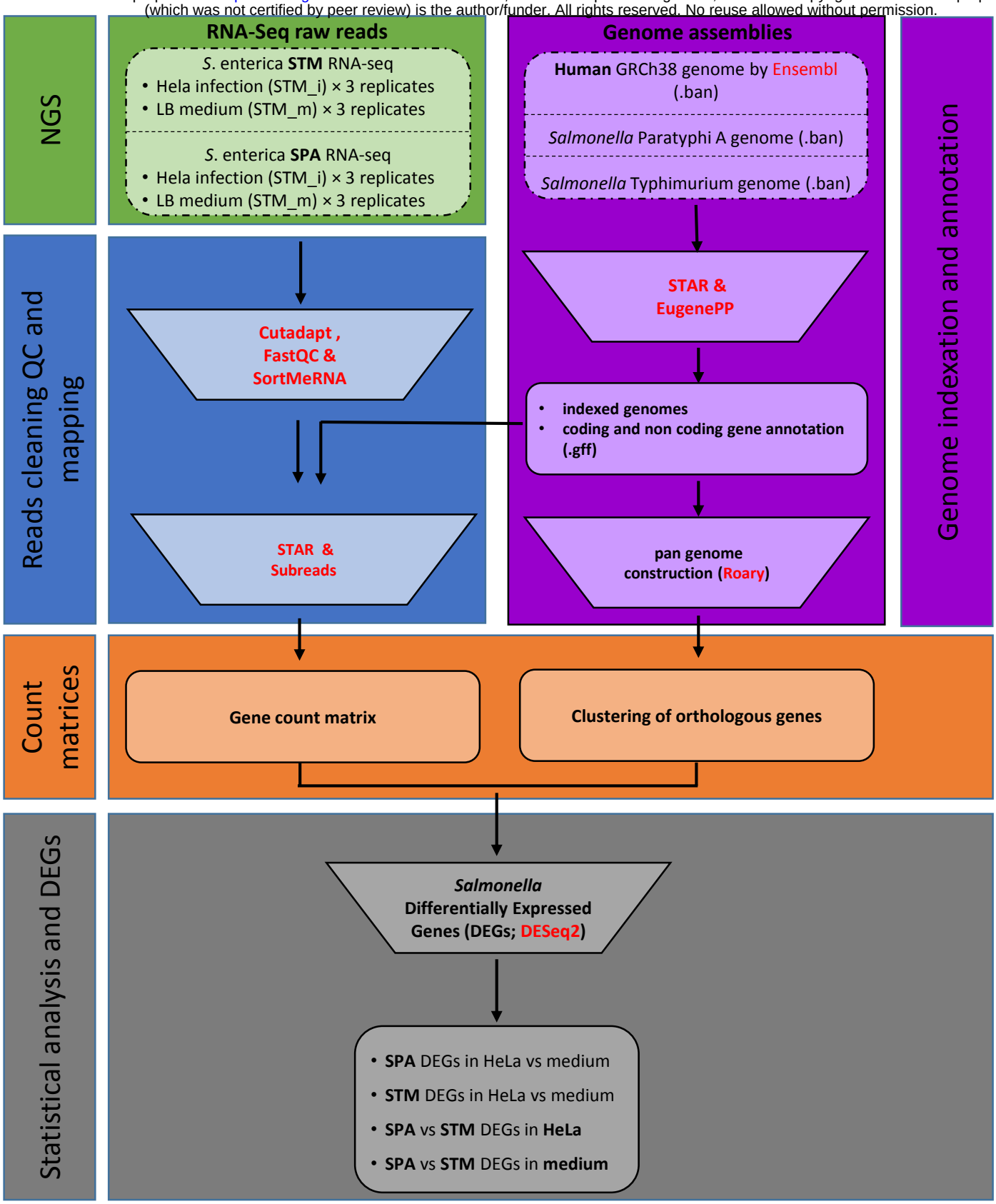

Fig. S4